



**UNIVERSITÀ DEGLI STUDI DI MILANO**

**FACOLTÀ DI MEDICINA E CHIRURGIA**

**DIPARTIMENTO DI SCIENZE BIOMEDICHE PER LA SALUTE**

**DOTTORATO DI RICERCA IN SCIENZE FISIOPATOLOGICHE, NEUROPSICOBIOLOGICHE**

**E ASSISTENZIALI DEL CICLO DELLA VITA - XXV CICLO**

**BIO16**

**THREE-DIMENSIONAL DENTAL IMAGING  
THROUGH VIRTUAL STUDY MODELS**

**TUTOR: PROF. CHIARELLA SFORZA**

**PRES. SCUOLA DI DOTTORATO: PROF. ROBERTO WEINSTEIN**

**TESI DI DOTTORATO DI  
LUIS TOMAS HUANCA GHISLANZONI  
MATR N° R08745**

**ANNO ACCADEMICO 2012-2013**

## **INDEX**

<b>CHAPTER 1 - GENERAL INTRODUCTION</b>	<b>1</b>
<b>CHAPTER 2 - NEW PERSPECTIVES ON THE USE OF THREE-DIMENSIONAL DENTAL MODELS IN ORTHODONTICS</b>	<b>5</b>
Introduction	6
From dental arches to three-dimensional files	7
The traditional use of 3D models: model storage and space analysis	8
The modern use of 3D models: virtual setup and longitudinal model comparison	9
The use of 3D models for research	9
The superimpositions problem	10
Conclusions	11
Figures	12
<b>CHAPTER 3 - EVALUATION OF TIP AND TORQUE ON VIRTUAL STUDY MODELS: A VALIDATION STUDY</b>	<b>16</b>
Introduction	17
Materials and Methods	18
Results	21
Discussion	22
Conclusions	23
Tables	24
Figures	26

<b>CHAPTER 4 - RAPID PALATAL EXPANSION EFFECTS ON MANDIBULAR TRANSVERSE DIMENSIONS MEASURED BY 3D DIGITAL IMAGING</b>	<b>28</b>
Introduction	29
Materials and Methods	29
Results	32
Discussion	33
Conclusions	35
Tables	36
Figures	38
<b>CHAPTER 5 - THE CONSTRUCTION OF THE AVERAGE ADULT UPPER DENTAL ARCH: A CLINICAL VALIDATION OF A NEW 3D METHOD</b>	<b>40</b>
Introduction	41
Materials and Methods	42
Results	44
Discussion	44
Conclusions	45
Tables	46
Figures	47
<b>CHAPTER 6 - GENERAL CONCLUSIONS</b>	<b>48</b>
<b>CHAPTER 7 - REFERENCES</b>	<b>50</b>
References	51
Index of abbreviations	57

# Chapter 1

---

## General introduction

## **GENERAL INTRODUCTION**

This thesis was conceived as a paper series analyzing the topic of three-dimensional dental imaging through virtual study models. The aim of the thesis was to explore some of the new possibilities of use of three-dimensional virtual study models as a modern diagnostic and research tool. At the time of writing the thesis chapter 2 to 5 have been adapted as papers and submitted to orthodontic journals for approval.

An abstract of each paper is presented here after, while in chapters 2 to 5 the details of each study are described. In chapter 6 general conclusions are presented, while in chapter 7 references for all the papers are reported.

### **NEW PERSPECTIVES ON THE USE OF THREE-DIMENSIONAL DENTAL MODELS IN ORTHODONTICS**

**Introduction:** Since orthodontic manufacturers managed three-dimensional models almost exclusively for a long time, orthodontists have a modest confidence with this imaging instrument. Times are ready for the use of three-dimensional virtual casts in everyday clinical practice and in research.

**Materials and methods:** In this paper the instruments to process a stone model into a virtual model are described. Possible advantages like storage of 3D files and the possibility of taking conventional measures (space analysis), are then discussed. Finally, the superimposition methods are discussed.

**Results and conclusions:** Clinical experience is the key factor when judging biological plausibility of dental movement imposed by a technician, when preparing a virtual setup. The possibility of superimposing virtual models opens unusual visual perspectives when comparing treatment results of a single patient or of a group of patients.

### **EVALUATION OF TIP AND TORQUE ON VIRTUAL STUDY MODELS: A VALIDATION STUDY**

**Objectives:** The objectives of this study were to develop and validate a custom digital dental analysis to measure linear and angular measurements of tip and torque of each tooth in

the dental arches.

**Materials and methods:** Maxillary and mandibular dental casts of 25 subjects with a full permanent dentition were scanned using a three-dimensional model scanner. Sixty points per arch were digitized on each model; five points on each tooth. A custom analysis to measure linear distances and angles of tip and torque was developed using a new reference plane passing as a best-fit among all of the lingual points, with the intermolar lingual distance set as reference X axis. The linear distances measured included buccal, lingual and centroid transverse widths at the level of canines, premolars and molars as well as arch depth and arch perimeter.

**Results:** There was no systematic error associated with the methodology used. ICC values were higher than 0.70 on every measure. The average random error in the maxilla was  $1.5^{\circ} \pm 0.4^{\circ}$  for torque,  $1.8^{\circ} \pm 0.5^{\circ}$  for tip, and  $0.4 \text{ mm} \pm 0.2 \text{ mm}$  for linear measurements. The average random error in the mandible was  $1.2^{\circ} \pm 0.3^{\circ}$  for torque,  $2.0^{\circ} \pm 0.8^{\circ}$  for tip, and  $0.1 \text{ mm} \pm 0.1 \text{ mm}$  for the linear measurements.

**Conclusion:** A custom dental analysis to measure traditional linear measurements as well as tip and torque angulation on virtual dental casts was presented. This validation study demonstrated that the digital analysis used in this study has adequate reproducibility, providing additional information and more accurate intra-arch measurements for clinical diagnosis and research.

## **RAPID PALATAL EXPANSION EFFECTS ON MANDIBULAR TRANSVERSE DIMENSIONS MEASURED BY 3D DIGITAL IMAGING**

**Objectives:** The purpose of this controlled study was to investigate indirect effects on mandibular arch dimensions, 1-year after Rapid Palatal Expansion (RPE) therapy.

**Materials and Methods:** Thirty-three patients in mixed dentition (mean age 8.8 y) showing unilateral posterior crossbite and maxillary deficiency were treated with a RPE (Rapid Palatal Expander, Haas type) cemented on the first permanent molars. Treatment protocol consisted of 2 turns per day until slight overcorrection of the molar transverse relationship occurred. The Haas expander was kept on the teeth as a passive retainer for an average of 7 months. Study models were taken prior (T1) and 15 months on average (T2) after expansion. A control group of 15 untreated subjects with maxillary deficiency (mean age 8.3 y) was also recorded with a 12 months interval. Stone cast were digitized with a 3D

scanner. Patients data were compared with data collected from the untreated group using t-tests. Correlations between variables were analysed with a linear regression model.

Results: In the treated group, both mandibular intermolar distance (+1.9 mm) and mandibular molars angulation (+9°) increased. Mandibular incisors angulation showed an increase of 1.9°. There was little effect on intercanine distance and canine angulation. Controls showed a reduction in transverse arch dimension and a decrease in molar and canine angulation values.

Conclusions: The RPE protocol has indirect widening effects on the mandibular incisors and first molars.

### **THE CONSTRUCTION OF THE AVERAGE ADULT UPPER DENTAL ARCH: A CLINICAL VALIDATION OF A NEW 3D METHOD**

Objectives: This article describes the digital construction and validation of an average adult upper dental arch and its application in the clinical environment.

Materials and Methods: A total of 24 upper dental arches of adult patients with a sound full permanent dentition, mean age 28.8 years (SD 5.6 yr), were selected for the study. 3D digital images of the dental casts were obtained with an optical laser-scanning device. The scanned images were analyzed using a three-dimensional visualization software. Seventy-nine landmarks were identified on each dental arch on the basis of a protocol previously validated for dental analysis. An average dental arch shell was then created and analyzed. Linear (tooth height and length, intermolar and intercanine distances) and angular measures (inclination of the tooth on a reference plane) deriving from the created average dental arch were compared with the average of measures deriving from single models using one-sample T-test ( $p < 0.05$ ). After validation, the average dental arch was used as a template for comparison with other dental arches presenting some form of malocclusion.

Results: The differences between the average upper dental arch and the average of single models were small (less than 0.1mm/1.0°) and not significant except for canine angulation. The linear measurements were highly precise. The angular measurements exhibited a higher, but acceptable, degree of precision.

Conclusions: The construction of the average dental arch is reliable and it can serve as a method for measuring changes in groups of patients or as a template for the comparison with arches showing malocclusion.

## **Chapter 2**

---

# **New perspectives on the use of 3D dental models in orthodontics**



## INTRODUCTION

Contemporary orthodontics have long embraced the third dimension,<sup>1</sup> both in clinics<sup>2-4</sup> and in diagnosis<sup>5</sup>.

Manufacturing industry financed private research to realize personalized and highly precise appliances (clear aligners, vestibular and lingual customized brackets).<sup>2-4,6</sup> A thorough knowledge of the 3D instruments and their use is essential to the orthodontist to understand the complex procedures of 3D image manipulation.<sup>7</sup> Such a knowledge allows the clinicians to interpret current research findings and give them the chance of a better interaction with the manufacturers representatives.

Research in the three-dimensional field has been almost exclusively oriented to Cone Beam Computerized Tomography (CBCT) imaging. The possibility of visualizing any aspect of the facial skull together with a low radiation dose excited the dental world. CBCT did not spread as much as expected, and nowadays its use is under study in many academic centers throughout the world. With CBCT it has become possible to visualize dental roots, included canines, skeletal anomalies and the “third dimension”, i.e. the transversal dimension, while orthodontists have been used to sagittal and vertical dimensions only for a long time.<sup>8-10</sup> It's still not clear if there's a net advantage in using CBCT instead of the traditional X-ray set (which exposes the patient to a smaller radiation dose). At the moment, the use of CBCT by the clinician is limited to those cases where a special anomaly requires further diagnostics.

Stereophotogrammetry followed CBCT in the interest of researchers.<sup>11,12</sup> Taking at least a couple photographs from different perspectives, it allows the creation of a 3D virtual image through a non-invasive method. This contemporary method strongly enhanced the study of the face. Anthropometry shifted from linear measurements to surface and volume measurements. Unfortunately, the stereophoto machines are highly expensive and are often prerogative of research centers.

With the exception of an initial enthusiasm for the first 3D scanners that converted plaster models into 3D images,<sup>13-15</sup> researches almost ignored the 3D dental model imaging. The introduction in the market of intraoral scanners arose a renovated interest around this topic.<sup>16,17</sup>

Storage on a hard disk and the possibility of automatized dental analysis have been claimed to be the major advantages of 3D virtual models as compared to traditional stone casts. There are many more advantages in using 3D virtual imaging. The aim of this thesis is to illustrate the new perspectives on the use of 3D dental models in orthodontics.

## FROM DENTAL ARCHES TO THREE-DIMENSIONAL FILES

Although research has proposed a set of tools to transform plaster models into three-dimensional images (holographic systems, laser technology, scanning for destruction, computed tomography),<sup>18,19</sup> laser scanning is the most common method to date (compact scanners are used in many orthodontic laboratories).<sup>15</sup>

The acquisition process involves placing the plaster model of the dental arch inside the scanner (Fig. 2.1). The model can be anchored to a rotary platform, or instead a rotating system of acquisition lenses, allows the dental arch to be recorded in its entirety, including undercuts.

Where the reproduction of the occlusal relationship with the opposing arch is necessary, a key of occlusion must be provided. This key can be a traditional chewing wax in maximum intercuspation, or even better, a silicone registration. An alternate way to reproduce the occlusion is bounding each other in maximum intercuspation the plaster models of the two opposing arches (for example, with a rubber band) and scan them simultaneously.

Many scanners can acquire three-dimensional images directly from impressions, without going through the development of a plaster model. In these cases, the precision of silicone impressions helps in achieving a good final quality of the virtual models. The accuracy of the impressions is the key to high-precision manufacturing (transparent aligners and vestibular or lingual custom brackets).<sup>20</sup> In the case of scanning directly from impressions, the only possible key of occlusion that can be provided is a wax or silicone bite registration.

Though it is still not popular, there is an opportunity with the intraoral scanner (Fig. 2.2) to completely skip the step of taking the impression in the traditional way. The intraoral scanner, typically mounted on modest-sized paddles, is able to scan directly in the mouth, transforming the dental arches into three-dimensional images that appear in real time on the screen.<sup>16</sup> In this case the key of occlusion is taken from the registration of the vestibular surface of the two dental arches in maximum intercuspation.

The most common and readable three-dimensional image format are .stl files. Not all scanners can save files in this format, because some companies prefer to store images in a proprietary format (linked to their software) and ask the orthodontist to pay a fee to convert the file into a universal format. It would be desirable to standardize the output in .stl files, as there is a wide range of free visualization software.

The three-dimensional surface is defined as mesh and consists of a large number of points,

linked together by small triangular surfaces, which are highly visible by zooming in on the surface of the model. The classic visualization favors a process of smoothing of the surfaces that transforms 3D models into a faithful screen replica of plaster models (Fig. 2.3).

## **THE TRADITIONAL USE OF 3D MODELS: MODEL STORAGE AND SPACE ANALYSIS**

One of the more tangible practical benefits of 3D models is the saving of physical space, as it is normal for the orthodontist to store initial and final models of their patients. The plaster casts can be abolished in favor of hard disk capacity. 3D files measure on average between 2 and 20 megabytes per dental arch, depending on the scanner used (smaller files with the same perceived quality are preferred). The proliferation of scanner models in many laboratories will make this method - in the near future - a common way of storing models. The laboratories that are already equipped with this technology upload files onto a dedicated server and provide login credentials to their customers, ensuring privacy and freeing them from the need to deliver the physical model in favor of a virtual delivery via e-mail. The exchange of medical records between colleagues is also facilitated electronically.<sup>21</sup>

National and international boards certifying the quality of orthodontic clinical treatment have, for the most part, already planned for the near future the integration of 3D models as valid clinical records alternatives to traditional plaster models.

The need to perform a space analysis is fully accomplished by 3D models; in fact, it is made easier.<sup>22,23</sup> It is not necessary to have a caliper, as this instrument is one of the basic tools provided in all 3D model visualization software. Some laboratories provide as a service a standard dental analysis of models (e.g. Bolton Index, space analysis), which frees the clinician from the need to perform these measurements personally. The literature has approved the correspondence between the measurements made in the traditional manner and with 3D models, declaring an equivalence, if not a slight superiority, in terms of accuracy in favor of the computerized method.<sup>22-24</sup>

## **THE MODERN USE OF 3D MODELS: VIRTUAL SETUP AND LONGITUDINAL MODEL COMPARISON**

The clinician who has had the opportunity to familiarize himself with the main suppliers of clear aligners has long been familiar with the concept of virtual setups. The virtual setup is a computerized version of the classic manual setup, saving a considerable amount of time for the technician. It is interesting how some providers of customized devices continue to prefer the manual setup, from which a three-dimensional scan is performed.<sup>6</sup>

The attention of the orthodontist, when delegating the setup to a technician who is not a clinician, must be concentrated on the plausibility of planned movements in the context of the patient's biological limits (anatomy, age, periodontium).<sup>25</sup> With a computer, it is in fact possible to simulate any type and any amount of movement.<sup>26</sup> It is not always easy to imagine the feasibility of these movements by displaying a sequence of two-dimensional images that show mild and progressive changes. Not even the direct comparison of before-and-after 2D images allows for such attention in this regard.

An exclusive feature of 3D models is the ability to superimpose (see separate section on the controversial issue of superimposition) and interpenetrate two different models. To perform this image processing, software is needed that compares the models (.stl) between them. The superimposition/ interpenetration of two differently colored models enables immediate and intuitive display of the teeth's positional changes. These changes are representative of before-vs.-after variations, where “after” can be both a virtual setup (with the purpose of verifying if the setup is adequate - Fig. 2.4) or the impression of the finished case (with the purpose of analyzing retrospectively the immediate changes of the dental arch – Fig. 2.5). The sharpness of the analysis can be amplified with the use of color scales (Fig. 2.6) that indicate the areas that have remained roughly unchanged (usually represented in green) and the areas where there has been movement in terms of enlargement (usually in blue) rather than contraction (usually in red).<sup>27</sup>

## **THE USE OF 3D MODELS FOR RESEARCH**

In terms of research, the analysis of classic models is based fundamentally on linear measurements and space analysis. With digital models the analysis can be enhanced with the ability to measure angles. It is therefore possible to measure the tip, torque, and rotations with a good degree of precision.<sup>28-30</sup> These “new” values can help us to better understand the

changes induced by the therapy or by growth. For example, ongoing studies have been made to try to understand the real effect of low-friction, expansive mechanics (Fig. 2.7): the possibility to calculate the torque permits the measurement of the degree of teeth flaring to the buccal.<sup>31</sup> In addition to linear and angular measurements, surface and volume measurements are also possible (e.g., palate surface and volume).<sup>32</sup> Increasing from one to three dimensions also increases the degree of measurement variability, and specific protocols must be validated on a case-by-case basis.<sup>33,34</sup>

Numerical analysis is helpful but visual image analysis is far more immediate.<sup>35</sup> The possibility of viewing the before/after changes of a patient's mouth was just mentioned. One can also extend this reasoning to a group of patients, as is already done when comparing cephalometric values. Instead of a numerical average to be compared, average arches can be produced that are representative of the sample under analysis. The procedure for creating three-dimensional images is complex and has been recently defined both for faces<sup>12</sup> and for dental arches,<sup>36</sup> and it will be discussed in chapter 5 of this thesis.

## **THE PROBLEM OF SUPERIMPOSING**

The possibility of superimposing for interpenetration of two dental models has already been mentioned. The criteria with which to match the arches were poorly described, and are often overlooked in the description of research protocols. It is, in fact, a controversial issue that deserves a mention.

As it is not possible to replicate invasive methods such the implant method used by Bjork to define ideal structures for superimposition in cephalometrics,<sup>37</sup> there has been an attempt to define areas with a low variability on which to perform "absolute" superimpositions on dental casts. In regards to the oral cavity, the only area of low variability is around the palatal rugae, in particular the more medial portion of the second and third rugae.<sup>38,39</sup> When applied to clinical cases, this knowledge revealed to be of little use because it takes into account only the upper arch, and because of the fact that the surfaces away from the palatal rugae are not finely superimposed (Fig. 2.8).

The main alternative superimposition method of dental models is the "best fit" method, i.e. the search for maximum correspondence between two models (the mutual relationship in which the standard deviation of the distances between the models is smaller, once the images have been superimposed on the centroid). This type of superimposition can occur in one or two steps. The first step is the identification of coinciding reference points on the models, and

then the subsequent application of a best-fit algorithm (prerogative of advanced software). To refine the superimposition the surfaces can be selected and the process of approximation models is relaunched (ICP method, or Iterative Closest Point): as the surfaces of the models consists of many points, the best fit of a the selected area is taken as the reference. This procedure is more precise and requires a greater calculation effort by the computer, since the procedure is repeated until the difference between the surfaces is minimized.<sup>40</sup>

Best-fit superimposition does not display absolute changes, but relative ones. It is therefore suitable to demonstrate changes in form and position. Absolute changes can only be viewed if the structures are free of biological remodeling processes, as is the case of mini-screws. The alternativivi would be to rely, with the identified limitations, on the superimposition of the palatal rugae.<sup>38</sup>

## **CONCLUSIONS**

Three-dimensional dental models can be proficiently used both as a diagnostic clinical record and as a research tool. The high cost of this technology limits its spreading in the orthodontic world. Nonetheless, as digital dental casts are prone to become a common tool in everyday practice, many other features, other than the one discussed in this chapter, will be described, as the third dimension allows to enter into unexplored paths of research.

## FIGURES

**Figure 2.1** - A compact scanner for 3D virtual model acquisition can stand on a desk, next to a laptop for data acquisition.



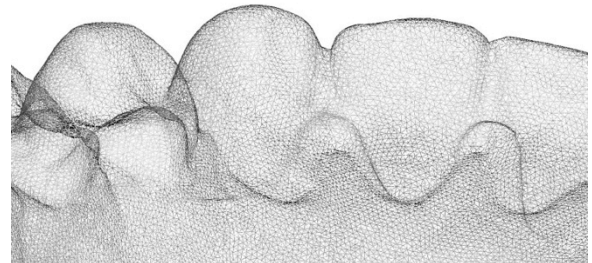
**Figure 2.2** - **A)** A sample of chairside intraoral scanner. **B)** A wand is used to replicate live-time the dental anatomy on the screen of a dedicated laptop.



**Figure 2.3 - A)** Classic visualization of a 3D virtual dental model with smoothed surface. **B)** Surface details: the precision of the surface is proportional to the density of the cloud of points that are linked together forming little triangles as the basic unit of the surface (mesh).

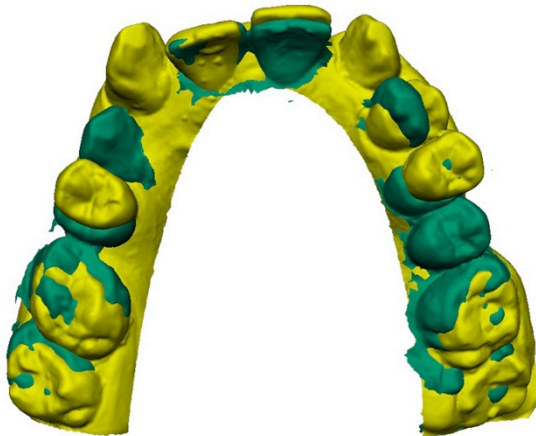


(A)

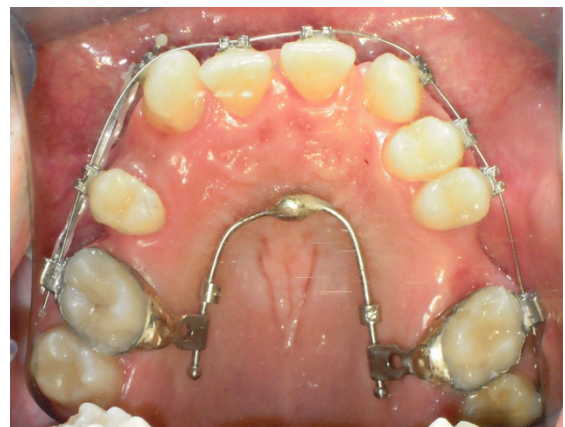


(B)

**Figure 2.4 - A)** Virtual setup to plan a complex case (yellow initial record, green setup). Through virtual setup it was possible to visualize the exact amount of expected distal movements that canines and premolars should perform. **B)** An appliance on miniscrew was then built to prevent excessive molar mesial movements, according to the virtual setup.



(A)



(B)



**Figure 2.5** – Superimposition of initial (white) and final (orange) virtual models of a patient treated to solve lower incisor crowding. It's easy to understand as the alignment occurred due to vestibularization of the lower incisors.

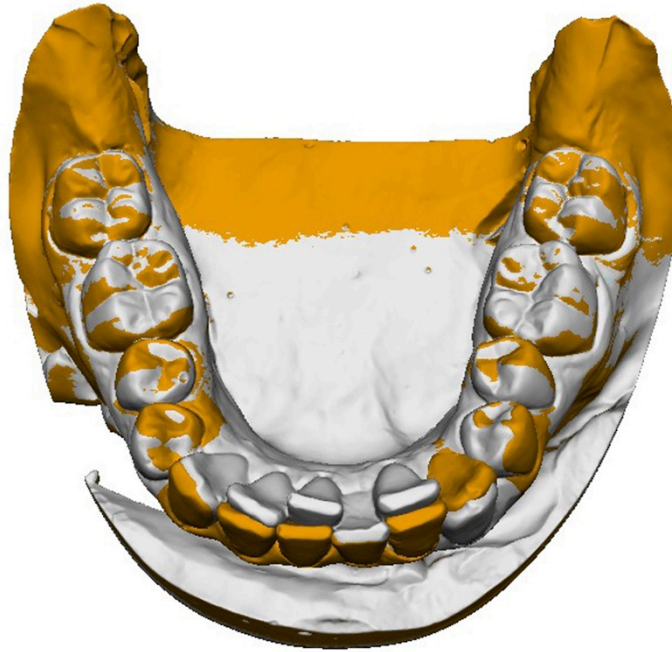
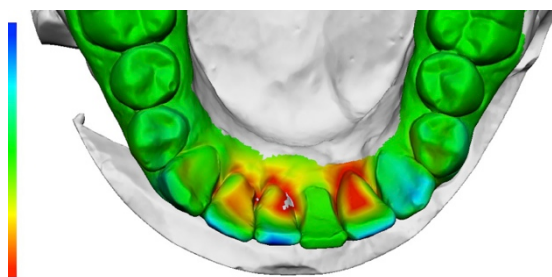
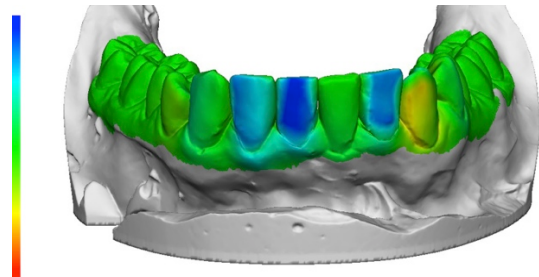


**Figure 2.6** - Colormap visualization of dental changes of the case showed in Fig. 3. In the color scale red represents -2 mm, green 0 mm or no change, blue +2 mm.

**A)** occlusal view. **B)** Frontal view.



(A)



(B)

**Figure 2.7** - Two mm coronal slice, cut at the level of the upper first premolar in a patient treated with low friction appliances and expansive mechanics (green initial, blue final). Virtual study models may help in understanding the real treatment outcomes in these cases (vestibularization or true expansion?).

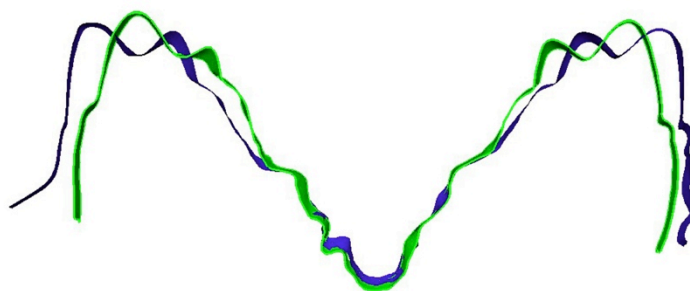
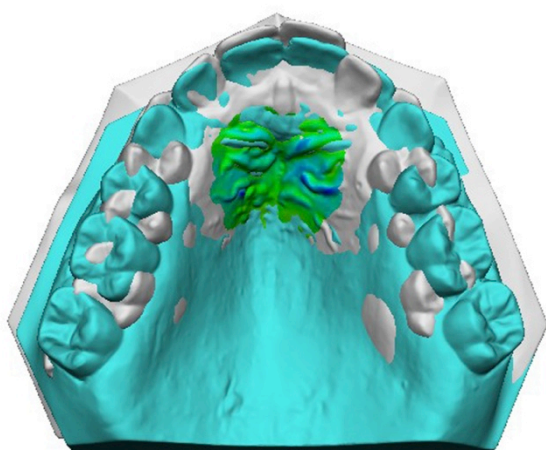
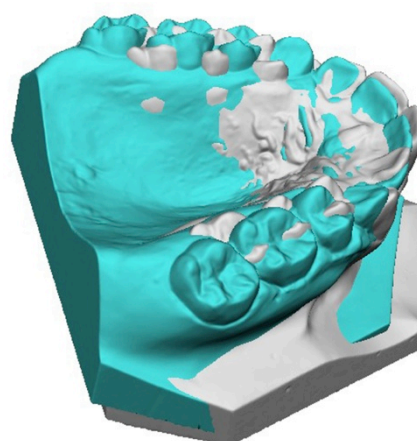


**Figure 2.8** - **A)** Superimposition on palatal rugae (green area) according to protocols described in the literature: an extraction case is showed (white initial, blue final). **B)** The superimposition at the molar level is poor (vertical displacement) as the molars are far from the superimposition area. The differences at the molar level are due to the limits of the superimposition method rather than to treatment outcomes.



(A)



(B)

## **Chapter 3**

---

# **Evaluation of Tip and Torque on virtual study models: a validation study**

## INTRODUCTION

The analysis of dental casts is an essential step in orthodontic diagnosis and treatment planning. A number of systems for on-screen measurements of virtual three-dimensional study models have been proposed in the literature to replace the time-consuming traditional manual measurements on plaster casts.<sup>15,22,24,41,42</sup> Three-dimensional (3D) virtual casts are an appropriate and accurate reproduction of the dental arch morphology for both indirect scanning systems from plaster casts and direct intraoral scanner acquisitions.<sup>43</sup> Digital measurements have proven to be as reliable as manual measurements with a caliper.<sup>15,22,24,41</sup> The digital dimension extends the diagnostic and research tools for both clinicians and researchers, allowing them to take measurements of angles of tip and torque, surfaces, and volumes.<sup>32</sup>

As orthodontists, we are concerned about the position of each individual tooth in the dental arches, including the angulation of the teeth in the mesiodistal dimension (tip) and in the faciolingual dimension (torque). Clinicians are continually faced with various tip and torque prescriptions of each commercially available bracket system, and often are unable to determine the extent to which the teeth follow the movement designated by the prescription. 3D virtual casts allow the use of additional tools to measure tip and torque, thus deepen the understanding of what happens to each tooth during treatment.

Through advances in manufacturing capabilities, today it is possible to build custom prescription brackets and aligners based on virtual setups of the dentition.<sup>19,20,25,26,29</sup> There have been attempts to measure intermolar and interincisal angles on plaster casts that have been trimmed, sectioned and photocopied; however, accuracy is difficult to achieve using this approach.<sup>44</sup> For example, questions have arisen regarding the accuracy of the work of Andrews<sup>45</sup> on tip and torque measured with a protractor because a repeatability test was not reported in his original work. More recent studies<sup>46-48</sup> repeated Andrews' work on different samples; however, their aim was to compare the findings on average tip and torque values rather than evaluating the accuracy of the methodology. Where reported, a fairly high range of variability (1.3 to 4.0 degrees) was found.<sup>47</sup>

Due to the irregular convexity of the facial surface of a tooth, it is difficult to measure the inclination reliably with the methodology used in previous studies.<sup>46</sup> Early attempts have been made to create a more precise custom analysis that provides tip and torque data by digital acquisition of points through a magnetic field.<sup>49</sup> These data do not reflect how orthodontists define tip and torque because the studies described the inclination of the Facial Axis of the

Clinical Crown (FACC) on an X and Y axes of a XYZ reference system. To measure the tip and the torque of each tooth requires a customized reference system.

The aims of the present study were to develop and validate a custom digital dental analysis to measure traditional linear measurements (e.g., transverse width, arch depth), as well as angular measurements of tip and torque of each tooth on virtual study models. Specifically, the validation of the analysis proposed in this study was performed to test its reproducibility as a diagnostic and research tool.

## **MATERIALS AND METHODS**

### **Subjects and methods**

Sample size was determined on the basis of a pilot study.<sup>50</sup> In order to detect an effect size of 0.6 for the average tip and torque angles, with a desired power of 0.80 and an alpha of 0.05, the sample size should be at least 24 dental casts. Maxillary and mandibular dental casts of 25 subjects (13 males, 12 females, age range 14-18 years) with a full permanent dentition up to the first molars, no dental anomalies or craniofacial syndromes, and no cast restorations or cuspal coverage, were selected from a parent sample of 60 subjects. The second molars often were absent or erupting and therefore were excluded from the analysis. In total, 25 maxillary dental arches and 25 mandibular dental arches from the same subjects were available to test the validity of the virtual analysis of the dentition.

The dental casts were scanned by way of the ESM/3ShapeTMR-700 three-dimensional model scanner (ESM Digital Solutions, Dublin, Ireland) and converted into .stl files. The VAM software (Vectra, Canfield Scientific, Fairfield, NJ) was used to edit the files by placing 60 points per arch, according to the following protocol.

### **Landmark digitization**

The 60 landmarks (Fig. 3.1) were digitized according to the following guidelines:

- Five points were taken for each tooth: the mesial and distal points of the occlusal surface, the gingival and occlusal limits of the buccal Facial Axis of the Clinical Crown (FACC),<sup>45</sup> and the gingival limit of the lingual FACC (continuation of the buccal FACC on the lingual surface).
- The most mesial and distal points of the occlusal surface of each tooth were digitized. The term occlusal surface is appropriate for molars and premolars, while for incisors it is represented by the incisal edge and for the canines by the canine ridges.

- For incisors, canines, and premolars, the buccal and lingual FACCs were identified three-dimensionally as the lines passing through the most prominent portion of the buccal surfaces and their projection onto the lingual surfaces. For molars, the buccal and lingual FACCs corresponded to the dominant vertical grooves on the buccal and lingual surfaces of the crown, respectively. Gingival and occlusal limits of both the buccal FACC and the gingival limit the lingual FACC then were digitized.

After checking for the consistency of point order,<sup>51</sup> the operator exported the points coordinates (XYZ) as a .txt file. Digitization of landmarks was repeated at a one month interval by the same operator to assess intraoperator repeatability. The data then were imported into Excel spreadsheets (Microsoft Excel, Microsoft, Redmond, WA) for the dental and statistical analysis.

### **Dental analysis**

A custom analysis to measure linear distances and angles was developed using a customized Excel file. The scanner allocated a random reference system to the digitized. It was thus necessary to re-establish a reference system related to the dental cast. The new reference plane for both maxillary and mandibular dental casts was calculated as the plane passing through the intersection of the lingual developmental groove of the first permanent molar with the gingival margin (gingival limits of the lingual FACCs of the molars) and the calculated centroid of the gingival limits of the lingual FACCs of all the teeth (excluding ectopic canines when that condition occurred).

The reference plane can be described as a best-fit plane among all of the lingual points, with the intermolar lingual distance set as the reference X axis. This reference plane was constructed nearly parallel to the occlusal plane, avoiding variability due to tooth position and torque, Curve of Spee, or Curve of Wilson (Fig. 3.2). The X axis represented the transverse dimension, the Y axis represented the sagittal dimension, and the Z axis (perpendicular to the XY plane) represented the vertical dimension. All points were converted to the new reference plane through a three dimensional rotational matrix.

Linear measurements were performed at this stage, while angular measurements required further computation.

### **Angular measurements**

*Torque* was measured as the labiolingual inclination of the and *tip* as the mesiodistal inclination of the FACC relative to the reference plane. An individual tooth coordinate system, which follows each tooth, was necessary to determine such values. The mesial and

distal points of each tooth were used for a second rotation of the XY plane, which determined the custom coordinate system for each tooth. The angles of torque and tip then were calculated using trigonometry. Lastly, a positive or negative sign was associated to the angle according to the same convention used for the brackets prescription (torque positive to the buccal and negative to the lingual, tip positive to the mesial and negative to the distal).

### **Linear measurements**

The measured linear distances included buccal, lingual and centroid transverse widths at the level of canines, premolars and molars as well as arch depth and arch perimeter.

Three different transverse dimensions were measured for each pair of homologous teeth from canines to first molars: the transverse vestibular distance (TV), the transverse lingual distance (TL), and the transverse bodily distance (TB). The TV was calculated as the distance between the occlusal limits of the buccal FACCs of homologous teeth. The TL was calculated as the distance between the gingival limits of the lingual FACCs of the homologous teeth. The TB was calculated as the distance between the three-dimensional centroids of the homologous teeth.

To determine the centroid of the canines, premolars and first molars, the midpoints of two lines passing from the mesial and distal landmarks (MD) and the gingival buccal and lingual limits of the FACCs (BL) were calculated. The midpoint of a line passing through these previously determined midpoints (MD and BL) then was determined. It was assumed that the centroid was the “center of mass” of the clinical crown.

Arch depth was determined by measuring the length of a perpendicular line constructed from the mesial contact point of the central incisors to a line connecting the mesial points of the first molars.<sup>52</sup> The mesial contact point of the central incisors was calculated as the midpoint between the mesial points of the central incisors.

Arch perimeter was calculated as the sum (on the XY plane) of six segments (three per quadrant) extending from the mesial point of first molars to the mesial point of first premolars, from the mesial point of the first premolars to the distal point of lateral incisors, and from the distal point of lateral incisors to the mesial contact point of the central incisors. Arch depth and arch perimeter were calculated as a projection of the defined segments on the horizontal plane (XY plane), as described in the literature.<sup>44,52</sup> Table 3.1 presents the entire set of measures.

## **Statistical analysis**

All dental casts for the 25 subjects were digitized twice by a single operator. The second digitization was repeated one month after the first digitization. Descriptive statistics were calculated for each linear and angular measurement at the 2 observation times. A normal distribution of the data of both the first and second acquisition was assessed through a Shapiro-Wilk test. A t-test for paired samples ( $p < 0.05$ ) was performed to assess the presence of systematic errors between the two observations.

Intraclass correlation coefficient with a two-way random effect model also was applied, checking for consistency between the 2 scores of the same rater. ICC values between 0.70 and 0.80 indicates a strong agreement, while values greater than 0.80 indicate an almost perfect agreement between the two observations. To assess for repeatability and consistency of the dental cast analysis, the method error was calculated through the “Method of Moments” Estimator (MME)<sup>53</sup> and the Relative Error Magnitude (REM).<sup>54</sup> The mean and standard deviation of the random error for torque, tip, and linear measurements of the maxilla and of the mandible were calculated.

## **RESULTS**

Table 3.1 and Table 3.2 report the statistics relative to the systematic and random error for each angular and linear value of the maxilla and of the mandible, respectively.

There was no systematic error; ICC values were higher than 0.70 on every measure.

The average random error in the maxilla was 1.5 degrees ( $\pm 0.4$  degrees) for torque measures and 1.8 degrees ( $\pm 0.5$  degrees) for tip measures. The average random error for the linear measurements in the maxilla was 0.4 mm ( $\pm 0.2$  mm).

The average random error in the mandible was 1.2 degrees ( $\pm 0.3$  degrees) for the torque measures and 2.0 degrees ( $\pm 0.8$  degrees) for the tip measures. The average random error for the linear measurements in the mandible was 0.1 mm ( $\pm 0.1$  mm).



## DISCUSSION

This study described and tested the reproducibility of a custom dental analysis performed on virtual three-dimensional study models. The shift from a standard “caliper and protractor” analysis to a virtual three-dimensional analysis allows the introduction of new tools and measures in addition to the classic linear measures (transverse dimensions, arch depth, and arch perimeter).

The procedure proposed by Andrews<sup>45</sup> for measuring the FACCs inclinations was time consuming and required numerous steps for measuring the angulations, and potentially was prone to error. According to the methodology proposed by Andrews, a “functional” occlusal plane needed to be chosen, with the cast trimmed parallel to this occlusal plane. A protractor then was used to measure the inclination of an axis tangent to a convex surface. This final step was the most controversial, because the definition of a tangent to a convex, irregular surface might lead to inaccurate measures.

Using a similar methodology, Richmond reported the range of error for the torque of the maxillary central incisors as 1.9 to 3.6 degrees.<sup>47</sup> With the custom 3D dental analysis presented in the current study, we found a method error that ranged from 1.0 to 2.0 degrees for the same teeth. The average method error of the torque values for all teeth was 1.2 degrees and 1.5 degrees for the mandible and the maxilla, respectively, while the error of tip values was 2.0 and 1.8 degrees for the mandible and the maxilla, respectively.

Ferrario and co-workers, using a mathematical approach similar to the one reported in the current study, digitized the landmark coordinates using an electromagnetic digitizer. These investigators reported a method error of 2.5 degrees and 2.3 degrees on the sagittal and frontal plane, respectively.<sup>49</sup> The linear measure error reported by Ferrario et al.<sup>49</sup> was 0.2 mm (calculated for the crown height length), while an average method error of 0.1 mm and 0.2 mm for the mandibular and maxillary linear measures, respectively, was reported in the current study.

The relative error magnitude in the present study ranged from 0.9% to 4.0% for the angular measures and 0.1% to 1.9% for the linear measures. Both the method error and the relative error magnitude indicate a good degree of reproducibility of both the linear and angular measures. The additional but necessary step of setting a custom reference system to calculate tip and torque angles may account for the higher degree of variation of the angular measures

when compared to the linear measures. Also, the error increases as the number of landmarks necessary for the measurement increases, as already reported by Luu et al.<sup>55</sup>

The definition of the tip and torque values as the actual inclination of a segment passing through the gingival and occlusal limits of the FACC may account for an improved reproducibility compared to manual measures with a protractor, as previously described in the literature.<sup>45-48</sup> The errors of the proposed method may be larger in longitudinal studies for comparisons of before- and after-treatment changes or in any clinical situation that potentially changes the clinical crown, both in the occlusogingival and the buccolingual dimensions. Examples include attrition of the occlusal surface due to bruxism, poor restorations, gingival inflammation, severe rotations, intrusion/extrusion biomechanics and teeth that are not fully erupted due to an early stage of maturation or a lack of space. The relative change of the gingival or occlusal limit of the FACC may account for an error in the estimation of the tooth inclination with respect to the reference plane.

The validation of the digital dental analysis in this study allows for the measurement of tip and torque and potentially can be applied to better understand the nuances of different bracket prescriptions. This new tool may be useful to both the clinician and the researcher as it may allow a better understanding of the changes that occur due to growth or to treatment when comparing dental casts at two different time points. Three-dimensional virtual dental cast analysis may be encouraged, as it provides additional information and more accurate intra-arch measurements than traditional stone cast analysis.

## **CONCLUSIONS**

A custom dental analysis to measure traditional linear measurements as well as tip and torque angulation was presented. This validation study demonstrated that the custom developed virtual dental cast analysis has adequate reproducibility, providing angular information (tip and torque) and more accurate intra-arch measurements for clinical diagnosis and research.

**TABLES**

**Table 3.1** - Statistics for the maxillary dentition. MME is the method error and its values are degrees for tip and torque, and mm for all the other measurements. RME is the relative error magnitude (%).

		T	ICC	MME	RME
torque	11	0.26	0.98	0.9	1.0
	12	0.56	0.98	1.2	1.3
	13	0.92	0.98	1.7	1.9
	14	0.18	0.94	1.6	2.1
	15	0.34	0.96	1.5	2.1
	16	0.98	0.87	1.7	2.3
	21	0.64	0.98	1.1	1.1
	22	0.88	0.98	2.2	2.4
	23	0.54	0.97	1.3	1.5
	24	0.72	0.96	2.2	2.9
	25	0.80	0.96	1.4	1.9
	26	0.86	0.92	1.5	2.1
	tip	11	0.90	0.92	2.0
12		0.49	0.94	1.4	1.5
13		0.12	0.90	1.5	1.6
14		0.96	0.84	1.6	1.7
15		0.45	0.81	1.8	2.0
16		0.05	0.90	1.5	1.6
21		0.89	0.89	1.6	1.7
22		0.07	0.93	1.3	1.3
23		0.14	0.94	2.6	2.7
24		0.51	0.92	1.5	1.6
25		0.41	0.78	2.2	2.4
26		0.80	0.72	2.8	3.0
3 to 3		TV	0.97	0.98	0.3
	TL	0.37	0.98	0.5	1.9
	TB	0.67	0.97	0.2	0.7
4 to 4	TV	0.90	0.99	0.5	1.4
	TL	0.63	0.99	0.4	1.5
	TB	0.23	1.00	0.4	1.2
5 to 5	TV	0.47	0.99	0.5	1.2
	TL	0.84	0.99	0.3	1.0
	TB	0.19	1.00	0.3	0.9
6 to 6	TV	0.95	0.98	0.2	0.5
	TL	0.08	1.00	0.2	0.6
	TB	0.09	0.99	0.2	0.5
arch depth		0.59	0.99	0.3	1.0
arch perim		0.60	1.00	0.8	1.1

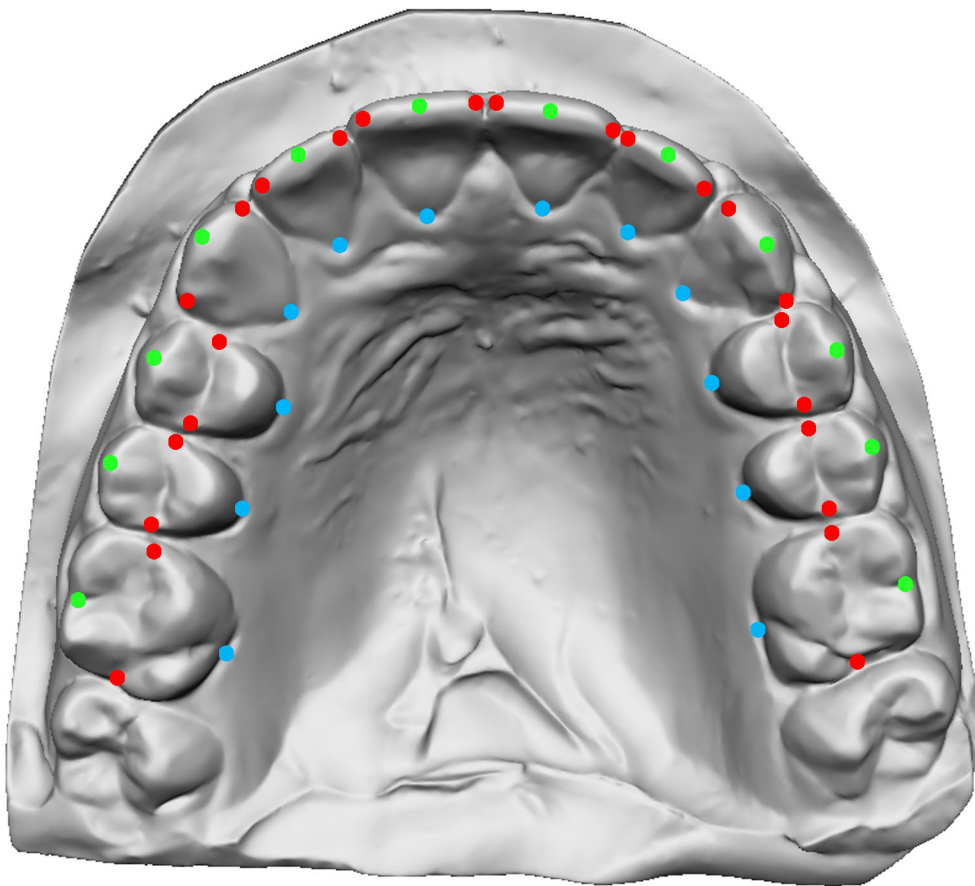
**Table 3.2** - Statistics for the mandibular dentition. MME is the method error and its values are degrees for tip and torque, and mm for all the other measurements. RME is the relative error magnitude (%).

		T	ICC	MME	RME
torque	31	0.24	0.98	0.8	0.9
	32	0.87	0.99	0.8	1.0
	33	0.96	0.97	1.2	1.7
	34	0.24	0.95	1.5	2.2
	35	0.84	0.98	1.2	2.1
	36	0.09	0.95	1.4	2.9
	41	0.17	0.98	0.9	1.0
	42	0.50	0.98	1.0	1.2
	43	0.45	0.96	1.2	1.6
	44	0.94	0.94	1.8	2.6
	45	0.29	0.98	1.1	1.8
	46	0.38	0.94	1.6	3.3
	tip	31	0.16	0.77	1.1
32		0.51	0.88	1.5	1.6
33		0.80	0.81	1.9	2.1
34		0.44	0.89	1.7	1.9
35		0.17	0.89	1.8	1.9
36		0.48	0.70	3.5	3.7
41		0.23	0.92	1.1	1.2
42		0.05	0.87	1.6	1.9
43		0.80	0.77	2.0	2.2
44		0.17	0.84	1.8	1.9
45		0.24	0.87	2.1	2.2
46		0.57	0.74	3.8	4.0
3 to 3		TV	0.83	0.96	0.2
	TL	0.97	0.91	0.2	0.9
	TB	0.85	0.96	0.1	0.3
4 to 4	TV	0.67	0.98	0.2	0.6
	TL	0.74	0.99	0.1	0.4
	TB	0.58	0.99	0.1	0.2
5 to 5	TV	0.30	0.98	0.1	0.3
	TL	0.61	0.98	0.1	0.3
	TB	0.38	0.99	0.1	0.2
6 to 6	TV	0.09	0.98	0.2	0.5
	TL	0.68	0.99	0.1	0.3
	TB	0.79	0.98	0.1	0.2
arch depth		0.13	0.98	0.1	0.4
arch perim		0.07	0.99	0.2	0.2

## FIGURES

**Figure 3.1** - A maxillary dental arch showing the distribution and the position of the 60 landmarks from an occlusal perspective (A) and on a lateral perspective (B). The red points are the mesial and distal points, the green points are the gingival and occlusal limits of the buccal FACC and the blue points are the gingival limits of the lingual FACC.

A)



B)

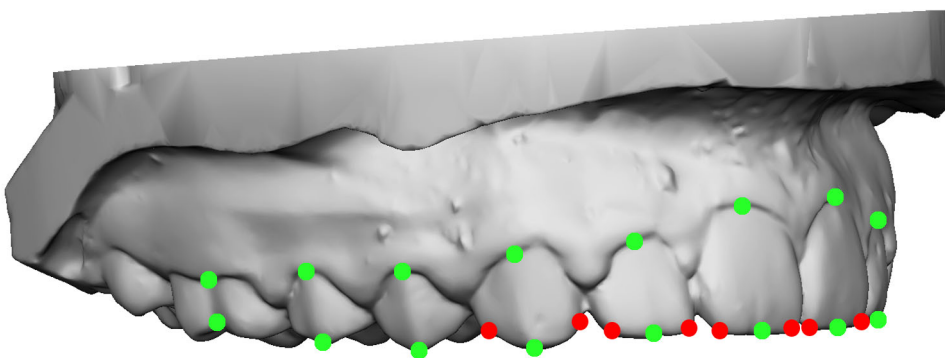
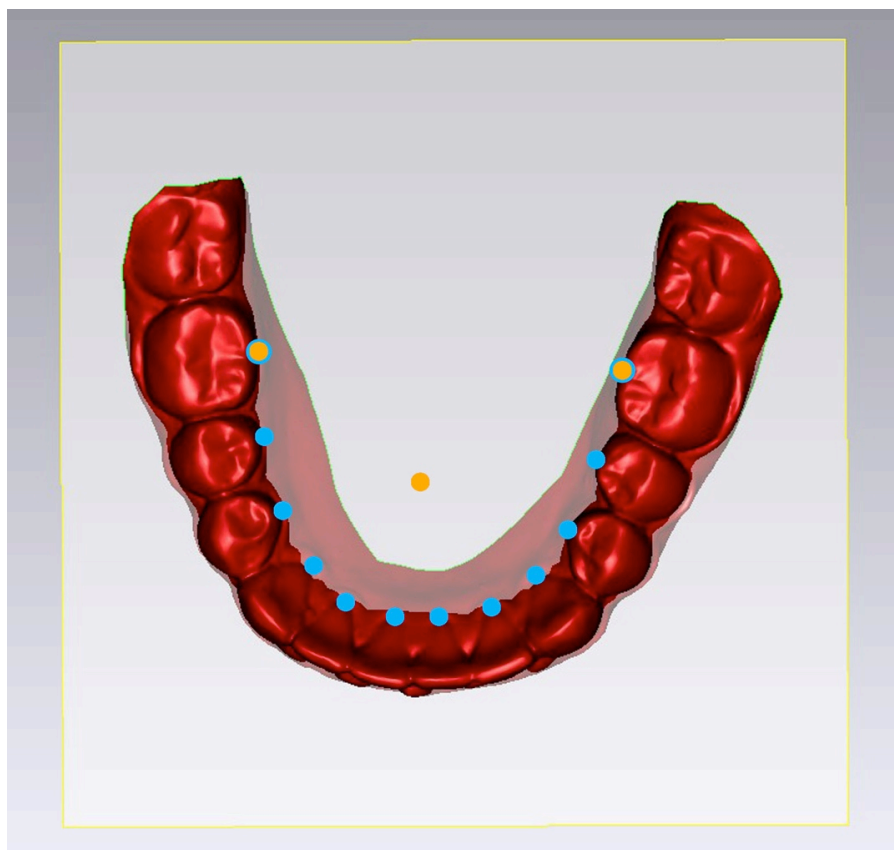
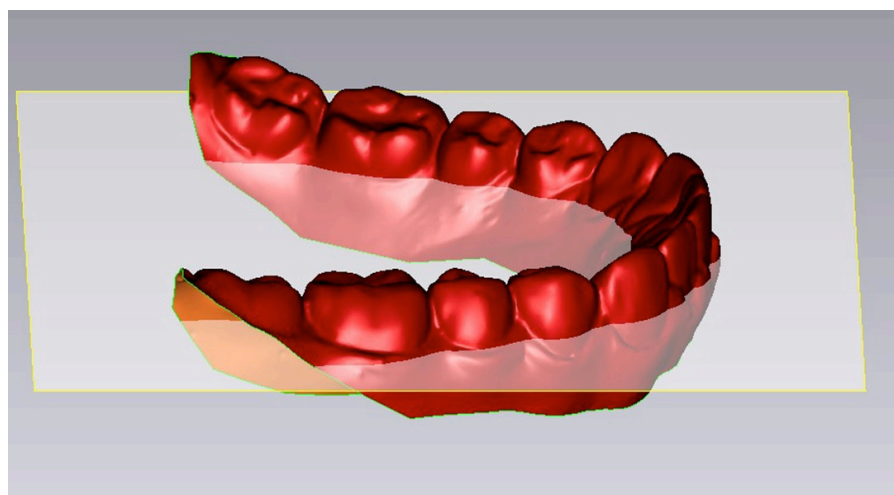


**Figure 3.2** - The reference plane is calculated as passing from the lingual molar points and the centroid (orange) of all the lingual points (blue) of the mandibular dental arch. An occlusal view (A) and a lateral view (B) are shown to understand the position of the plane in relation to the dental arch.

A)



B)



## **Chapter 4**

---

# **Rapid palatal expansion effects on mandibular transverse dimensions measured by 3D digital imaging**

## **INTRODUCTION**

Posterior crossbite is one of the most prevalent malocclusions in the primary and early mixed dentition and it is reported to occur in 8% to 22% of the general children population.<sup>56,57</sup> It occurs when the maxillary back teeth bite inside the mandibular back teeth. Posterior crossbite may develop or improve at any time from when the deciduous teeth come into the mouth to when the permanent teeth come through. If the crossbite affects one side of the mouth only, the mandible may need to move asymmetrically to allow the posterior teeth to meet together. This movement may have long term effects on the growth of the teeth and jaws. The subsequent neuromuscular adaptation to the acquired mandibular position can cause asymmetric mandibular growth, facial disharmony, and several functional changes in the masticatory muscles and temporomandibular joint (TMJ).<sup>58</sup> It is unclear what causes posterior crossbites but they may be due to skeletal, soft tissue, dental, or respiratory factors or develop as the result of a habit, e.g. thumb sucking or some pathology. For this reason several treatments have been recommended to correct posterior crossbite.

McNamara has speculated that the position of the mandibular dentition might be influenced more by maxillary skeletal morphology than by the size and shape of the mandible.<sup>59</sup> This hypothesis could explain why some mandibular arch decompensation happened during rapid maxillary expansion therapy, but very few published researches support this thesis.<sup>60-65</sup> While some recent investigations reviewed the palatal expansion and its effects on the palatal vault and the lower third of the face in a three-dimensional perspective, an evaluation of the effects on the mandible with a 3-d non invasive analysis is still missing.<sup>66,67</sup>

The primary focus of the current study was the assessment of the spontaneous mandibular response after Rapid Palatal Expansion (RPE) therapy, in patients with unilateral cross-bite, as measured from three-dimensional digital dental models.

## **MATERIAL AND METHODS**

### **Subjects**

Forty-eight patients with posterior crossbite were consecutively selected. The patients were treated at the Department of Orthodontics, University of Siena (Italy) and in a private practice in Genoa (Italy) between 2006 and 2009 and were selected according to the following



inclusion criteria:

- early or mid mixed dentition stage;
- cervical vertebral stage 1 through 3 (CVS method 1–3);<sup>68</sup>
- unilateral posterior crossbite;
- Angle Class I or Class II malocclusion;
- underwent RPE banded (Haas type) therapy (RPE, treated group);
- or, to be submitted to RPE banded (Haas type) therapy (control group);
- no subsequent comprehensive orthodontic treatment implemented in either the maxilla or the mandible.

The RPE group consisted of 18 girls and 15 boys; average age at T1 was 8.8 years (SD 1.1 years). The control group consisted of 8 girls and 7 boys; average age at T1 was 8.3 (SD 1.2 years). These patients were matched for age, sex and skeletal maturity with the RPE groups but did not receive any orthodontic treatment, and their dental casts were taken a second time after approximately 12 months.

In the RPE group, the records included pre-treatment (T1, immediately before the cementation of the appliance) and post-treatment dental casts (T2, after the appliance was removed and replaced by a removable plate, 15 months interval on average).

All palatal expanders (tooth-tissue-supported, Haas type) were manufactured, cemented, and activated according to the following protocol: at initial activation, the appliances received 2 quarter turns (0.4 mm). Thereafter, the appliance was activated 1 quarter turn in the morning and 1 quarter turn in the evening. The subjects were seen at weekly intervals for approximately 3 weeks. When the desired overcorrection for each patient was achieved, the appliance was stabilized. The expander was in situ during the expansion and stabilization period for a mean time of 7 months (range 5-9 months). After removal of the expander, a loose, removable acrylic plate was delivered within 48 hours.

### **Cast Analysis**

The sample consisted of 96 cast models which were scanned by a D640 scanner (3Shape, Copenhagen, DK): 3D digital model (\*.stl) were thus obtained.

3D digital model processing and cast analysis were accomplished with a multi-step procedure. The first step consisted of landmark digitization on each model through VAM application version 2.8.3 (Canfield Scientific Inc, Fairfield-NJ, US). A protocol similar to the one developed by Ferrario et al.<sup>49</sup> was followed (see also to chapter 3 of this thesis). Dental landmarks were identified on screen on the scanned mandibular dental casts. When either

the deciduous teeth were missing or the permanent teeth were not fully erupted, the measurements for that variable were eliminated. For each patient a total of 15 mandibular landmarks were digitized. Two landmarks per teeth allowed to trace the Facial Axis of the Clinical Crown (FACC) of the first permanent molars, deciduous canines and permanent central incisors, at T1 and at T2. Mandibular reference planes were computed between the incisive papilla and the intersections of lingual sulci of the first permanent molars with the gingival margin (Fig. 4.1a and 4.1b). Lingual measurements for mandibular intermolar width were obtained at the point of the intersection of the lingual groove with the cervical gingival margin, according to McDougall et al.<sup>15</sup> The occlusal intermolar width was measured as the distance between the mesiobuccal cusp tips of the first permanent molars bilaterally; the intercanine width was the distance between cusp tips bilaterally. Mandibular first molar, canine and incisor angulations were calculated as the angle of projection of the facial axis of the clinical crown (FACC) on the reference plane (a positive value stands for vestibularization).

The whole set of landmarks was exported into a .txt file. The .txt file was imported into an Excel matrix, and x, y and z coordinates were divided into three columns.

The 3D point set was re-orientated putting the reference lingual plane parallel to the xy plane. Finally the data set was analyzed with a custom excel procedure for 3D arch analysis. The process was repeated for each mandibular arch cast (Fig. 4.1a and 4.1b).

### **Method error**

To standardize measurements, all data were collected by an investigator. Measurements were repeated on 10 randomly selected casts to determine the error of the method between the first and second measures. Intraclass correlation coefficients were calculated to compare within-subjects variability to between-subjects variability; all values were larger than 0.95. Standard deviations between repeated measurements were found to be in the range of 0.08 to 0.17 mm for all measurements (average variation, 0.1 mm). Overall, the method error was considered negligible.

### **Statistical Analysis**

Descriptive statistics were computed for all analyzed variables: occlusal and lingual intermolar distances; intercanine distance; left and right molar, canine and central incisors angulation values; molar, canine and incisors mean values (i.e. right and left average angulation values).

Shapiro-Wilks test showed that data were normally distributed, and parametric statistics

were applied. Patient (RPE group) data were compared with the data collected from the untreated group using Student's t-tests. Probabilities of less than 0.05 were accepted as significant in all statistical analyses. Sample size was calculated a priori to obtain a statistical power of the study greater than 0.85 at an alpha of 0.05, using the mean values and standard deviations of mandibular molar expansion after RPE therapy found by Lima et al.<sup>62</sup>

The effects size (ES) coefficient was also calculated.<sup>69</sup> For Cohen's *d* an effect size of 0.2 to 0.3 might be a "small" effect, around 0.5 a "medium" effect and 0.8 to infinity, a "large" effect.

A linear regression model was employed to assess correlations between treatment duration (months of therapy, MOT) and mandibular dental angulation values.

## RESULTS

Descriptive analyses of the mandibular variables at two assessment stages for all 48 subjects are shown in Tables 4.1 and 4.2, and figure 4.2. It was possible to measure only fully erupted teeth (permanent or deciduous). Therefore, for some measurements a reduced number of subjects was analyzed (Table 4.1). No differences between groups were found at T1. At T2, all patients had their crossbite corrected. No spontaneous crossbite corrections were observed in the control group.

The net changes of the T1-T2 interval are reported in Table 2. In treated subjects, mandibular intermolar distance significantly increased 1.9 mm on the vestibular side and 0.7 mm on the lingual side. Mandibular molar angulation increased 9°. There was a significant but little effect on mandibular incisors angulation (+1.9°), intercanine distance (+1.0 mm) and on canine angulation (+5.1°). Control subjects showed a tendency towards contraction of the transverse dimensions and a decrease in molar, canine and inferior incisor angulation values.

ES coefficients were also calculated and are listed in Table 2. These variables (36-46 occlusal, 36-46 lingual, 33-43, Molar angulation, Canine Angulation, Incisors Angulation) were characterized by a significant, medium or large, effect size.

Linear regression between MOT and mandibular first molar angulation showed a significant correlation ( $p = 0.02$ ;  $y = 0.529x - 2.050$ ,  $R^2 = 0.441$ ), while no correlations between MOT and mandibular central incisor and canine angulations were found.

## DISCUSSION

All subjects were selected before the pubertal peak (CVS 1–3), because Baccetti et al. showed that in these 3 stages RPE patients exhibit significant and more effective long-term changes at the skeletal level in both maxillary and circummaxillary structures.<sup>68,70</sup> A control group of untreated patients with the same malocclusion was also used to identify confounding factors such as natural craniofacial growth and development during the study period.

A few data were found in biomedical literature about the RPE effects on mandibular molar, canine and incisors angulation.<sup>65</sup> Otherwise, no data about changes in mandibular arch angulation in untreated unilateral cross-bite malocclusion were reported in previous studies. In the current investigation, normal transversal arch growth was modified by cross-bite malocclusion: the patients showed a tendency towards contraction of the transverse mandibular dimension and a decrease in molar, canine and incisor angulation values. Previous longitudinal investigations found a slight but continue decrease in the intercanine width (0.5-1.5 mm) during the maturation of the permanent dentition.<sup>71–73</sup> Moorrees and Reed showed the intercanine width does not change from the age of 8 to 10 years and the mandibular intermolar width increases 3 - 4 mm from 6 to 17 years of age.<sup>74</sup> Two long-term retrospective trials, by Geran et al. and O'Grady et al., reported the changes in untreated (Class I or Class II malocclusion but not cross-bite) control groups.<sup>63,64</sup> They found a reduction in mandibular arch perimeter, mainly related to the exfoliation of the mandibular second deciduous molars; a slight decrease in intercanine width and a very little or no increase in molar width. Unfortunately, the time interval (T1-T2) for decrements reported by Geran et al. for their control group was 5 years, and it cannot be directly compared to our time interval.<sup>63</sup>

When compared to the untreated group, the present RPE group showed significant net increases of intermolar width from pre-expansion (T1) to follow-up (T2): 1.9 mm, occlusal value, and 0.7 mm, lingual value. These increases were greater than some of the mandibular intermolar widths (occlusal) previously reported. Several authors reported an increase in mandibular molar width ranging from 0.24 to 2.8 mm.<sup>60,61,75,76</sup> Wertz evaluated 48 patients for mandibular intermolar width changes after 3-4 month of RPE therapy (plus stabilization) and found 35 patients of 48 with no change, 12 of 48 with increases of 0.5 to 2.0 mm, and 1 of 48 with a decrease of 1.0 mm, but that study were included children, teenagers and adults.<sup>75</sup> Moussa et al.<sup>60</sup> and Sandstrom et al.<sup>76</sup> evaluated mandibular intermolar width change after RPE, but their patients also underwent fixed appliance therapy, and they are not directly comparable to our study.

From T1 to T2, both above mentioned increases suggest a slight first molar uprighting. This hypothesis is confirmed by the angulation values. From T1 to T2 the inferior first molar angulation was significantly increased,  $+8.8^\circ$ . In a recent study, Lima et al., found that mandibular intermolar arch width increased significantly after RPE with a Haas-type expansion appliance and that the increase was followed by a slight decrease of the occlusal value, whereas the lingual value was maintained, thus suggesting a tendency to lingual angulation in the long term.<sup>62</sup> For intercanine width (occlusal value), we found a little effect on intercanine distance (+ 1.0 mm) but not on canine angulation. Similar results were reported by Lima et al.<sup>7</sup> Haas reported no change for intercanine width in 5 of 10 analyzed subjects; however, the age range was significant higher than in the present study.<sup>77</sup> All short-term and long-term studies, as reviewed by Lima et al., showed very different value for intercanine width increases, ranging from 0.5 to 5.0 mm, which might be attributed to differences in sample selection criteria.<sup>62</sup> Lagravere et. al.<sup>78</sup> reported that most of the mandibular intermolar increments noted immediately after RPE was not statistically significant.

Baysal et al. evaluated the post RPE changes in mandibular arch widths and buccolingual inclinations of mandibular posterior teeth by using CBCT images. They measured linear and angular changes in mandibular posterior region, and after 6 months they found an increase of the axial inclinations of all mandibular posterior teeth and of the mandibular transversal dimension.<sup>65</sup> There is a good accord between the current and the study by Baysal et al., and data are directly comparable, due to the similar 3D measurements. Thanks to our 3D cast analysis system, we can record the same variables using non-invasive procedures.

In the present study, RPE therapy allowed an increment in mandibular arch transversal dimensions and an increase in molar, canine and incisors angulations. Angulation increase may result from two different biomechanical effects, postulated by Haas.<sup>77</sup> The first is an occlusal change. The direction of occlusal forces is altered by the maxillary expansion, so that the resultant force vector acting on the mandibular teeth (especially molars) is more vestibularly directed, because the occlusal aspect of the lingual cusp of upper first molars contacts the occlusal aspect of the facial cusp of the lower first molars. The second is a “lip bumper effect”: the lateral movement of the maxillae widened the area of attachment of the buccal musculature.<sup>65</sup> These theses were indirectly supported by the correlation between molar angulation increase and months of therapy.

Although long-term longitudinal data are needed, the present study's sample size, along with the significant effect size of the difference in the decompensation of mandibular arch, enforce the statistical significance of the outcomes.

## **CONCLUSIONS**

Mandibular intermolar arch width increased significantly after RPE with a Haas-type expansion appliance. This increase was followed by a significant increase of molar angulation. There was a significant but little effect on intercanine distance and on canine and incisors angulations. The positive clinical effect in mandibular arch-width dimensions in patients treated only with RPE is consistent with a spontaneous mandibular arch response to RPE.

RPE therapy had widening indirect effects on the mandibular first molars, canines and incisors, at one year follow up. The values of Cohen's of Effect Size confirmed the clinical indirect effects of RPE on mandibular arch. The molar angulation value increase was correlated with the months of RPE therapy.

## TABLES

**Table 4.1** - Descriptive statistics and comparisons between groups at T1.

Variable	Unit	Control Group			RME Group		
		N	Mean	SD	N	Mean	SD
Age	years	15	8.3	1.2	33	8.8	1.1
T1-T2	months	15	12	2.4	33	15	2.4
36-46 (occlusal)	mm	15	46.9	2.4	33	47.1	2.9
36-46 (lingual)	mm	15	33.7	1.7	33	33.5	2.4
33-43	mm	14	27.0	1.5	16	26.5	2.0
36 angulation	°	15	-44.7	6.8	33	-47.6	8.8
46 angulation	°	15	-44.7	10.7	33	-48.4	6.9
33 angulation	°	13	-13.7	6.8	20	-15.8	6.8
43 angulation	°	13	-16.3	8.9	20	-17.1	12.0
31 angulation	°	15	-8.1	4.8	25	-9.0	6.2
41 angulation	°	15	-7.7	5.4	25	-8.7	7.6

All comparisons were not significant ( $p > 0.05$ , Student's t test for independent samples)

**Table 4.2** - Mean and standard deviation (SD) of the differences between T2 and T1 values for each patient.

	Control Group		RME Group		Diff T2-T1	T Test	Effect Size		
	unit	Mean	SD	Mean			SD	p value	d value
36-46 (occlusal)	mm	-0.8	0.8	1.1	1.5	1.9	0.00	0.6	Large
36-46 (lingual)	mm	-0.1	0.4	0.6	1.2	0.7	0.00	0.8	Large
33-43	mm	-0.6	0.8	0.4	1.6	1.0	0.01	0.4	Medium
36 angulation	°	-3.3	5.2	6.2	5.8	9.5	0.00		
33 angulation	°	-6.0	5.0	0.7	5.5	6.7	0.00		
43 angulation	°	-2.7	6.6	0.7	7.4	3.4	ns		
46 angulation	°	-3.8	5.7	4.3	6.8	8.1	0.00		
31 angulation	°	-2.5	4.0	2.0	4.1	4.4	0.00		
41 angulation	°	-2.4	3.5	1.8	3.1	4.2	0.00		
Molar angulation (mean)	°	-3.5	5.5	5.2	6.3	8.8	0.00	0.6	Large
Canine angulation (mean)	°	-4.4	5.8	0.7	6.4	5.1	0.01	0.4	Medium
Incisor angulation (mean)	°	-2.4	3.7	1.9	3.6	4.3	0.00	0.5	Medium

Diff. T2-T1: Mean differences between RME and Control groups. ns: not significant,  $p > 0.05$

d: Cohen's effect size value

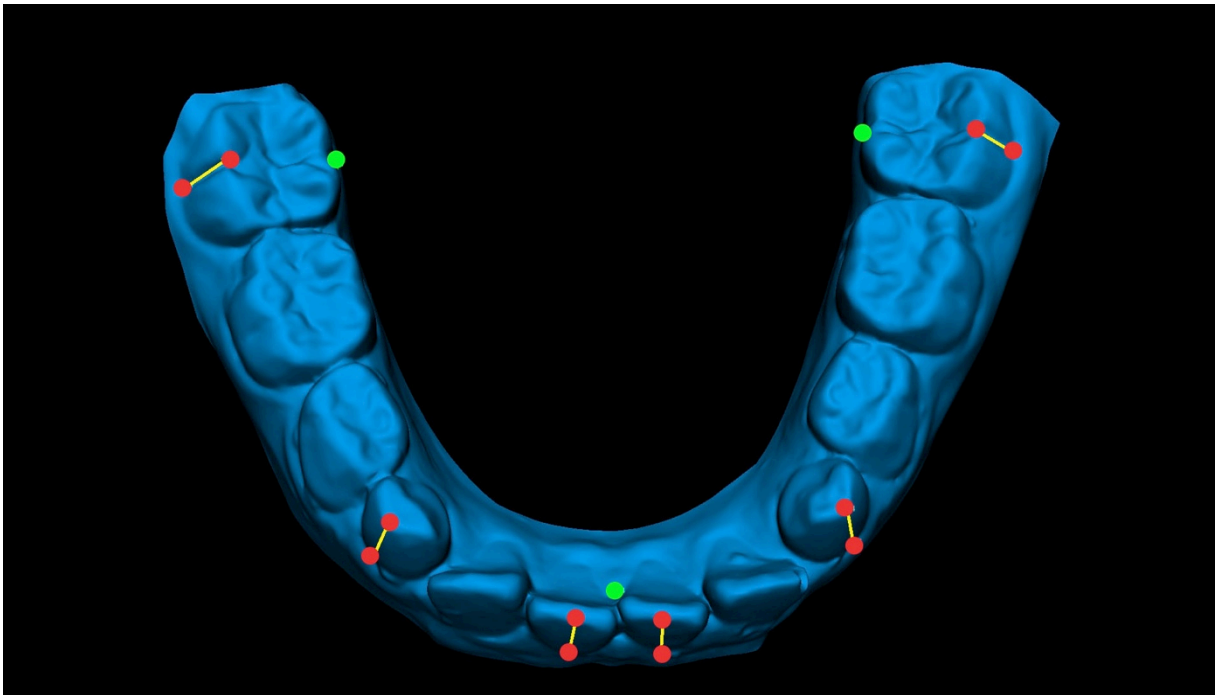
ES: effect size



## FIGURES

**Figure 4.1** - Digital mandibular model with markers: dental markers in red, reference plane markers in green. A) FACC, used to calculate angulation, in yellow. B) intercanine and intermolar (lingual and vestibular) distances in white.

A)



B)

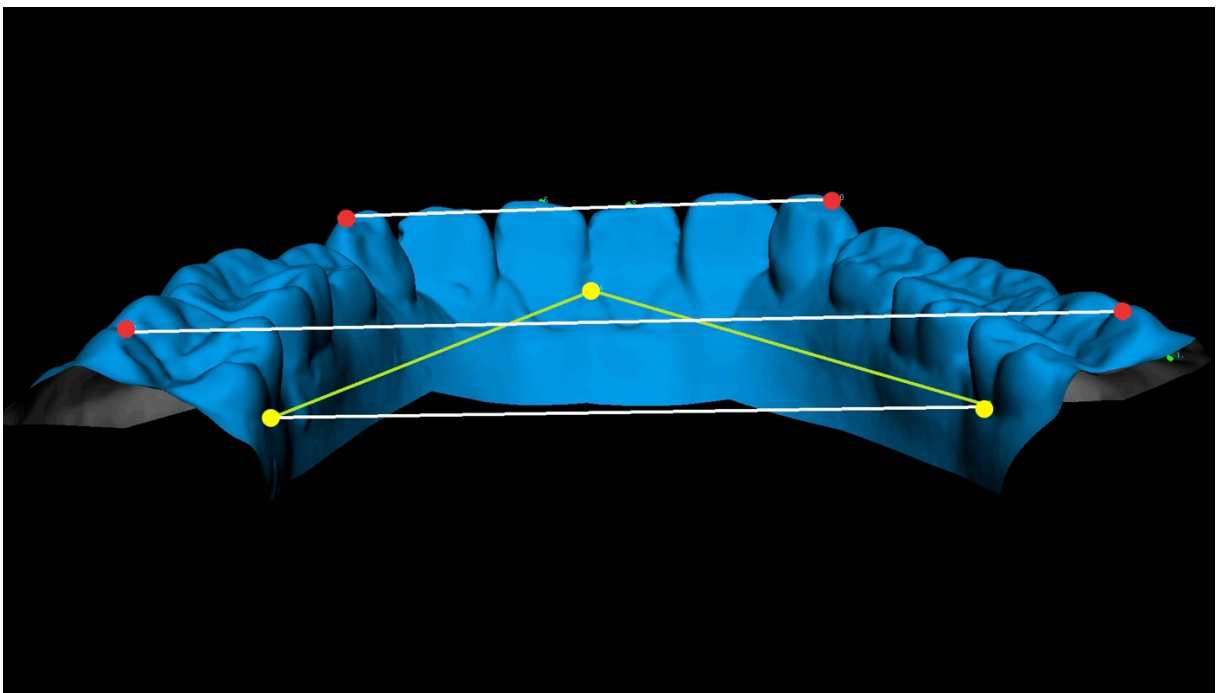
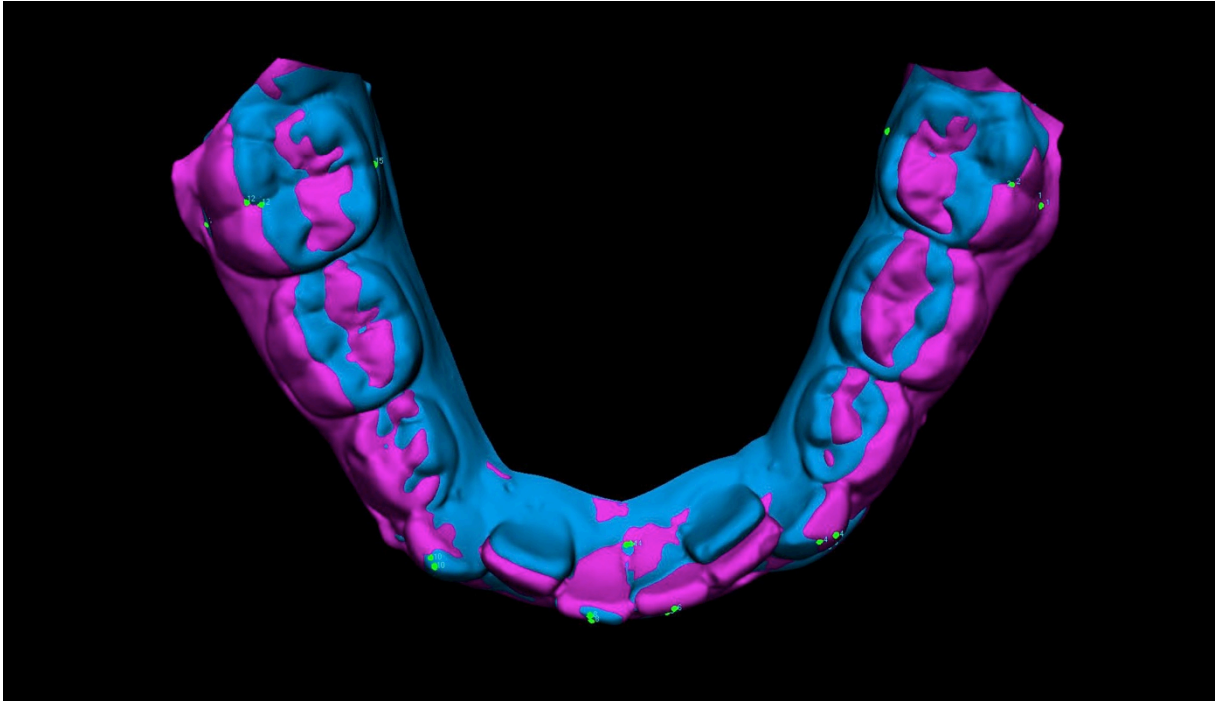


**Figure 4.2** - Superimposition of pre- and post-treatment digital models of the mandible shown as example of mandibular response to RPE treatment.



## **Chapter 5**

---

# **The construction of the Average adult upper Dental Arch: a clinical validation of a new 3D method**

## INTRODUCTION

Dental cast analysis is one of the main focus of orthodontic diagnosis.<sup>79</sup> In a general trend toward a three-dimensional (3D) visualization of orthodontic diagnostic data, the dental images appear to have fallen behind compared to facial (stereophotogrammetry, laser scan)<sup>12,80-83</sup> and bone (cone beam tomography)<sup>5,84-86</sup> images.

Measurements on digital dental models were found to be comparable to those on plaster models.<sup>23,55,87-89</sup> According to some Authors,<sup>23,90</sup> digital models can be even better than plaster models since they allow a wider view when placing landmarks. While it is relatively easy to find in the literature papers regarding digital dental model analysis<sup>35,87,88</sup> and visual superimposition applied to single patients,<sup>35,91</sup> it is quite hard to find any other applications.

In orthodontics, superimpositions of lateral headfilm tracing on stable structures is still the commonest mean of evaluating the treatment effects of a specific therapy.<sup>92</sup> Cephalometric superimposition appears to be very effective in defining changes in bone shape and size in a two-dimension perspective (sagittal plane projection)<sup>92</sup> while it is less precise in measuring changes of the teeth and of the soft-tissues. For instance, this method can show positional changes of the maxillary and mandibular dentition in both vertical and sagittal dimensions but not buccopalatal crown movement.

Stereophotogrammetry and laser scanning can be considered the best ways to assess soft-tissue changes as they provide a huge amount of details of the face using efficient and non-invasive procedures and also without the risks of radiation exposure. A method for superimpositions of the 3D face shells has been described and validated by Kau et Al.<sup>12,81</sup> They also defined a protocol for the creation of the average face<sup>12</sup> and then used it as a reference to measure ethnic differences in groups of individuals<sup>80,83</sup> or as a template for the comparison of facial disproportion.<sup>82,93</sup>

A similar approach would be highly desirable for studying teeth movements before and after an orthodontic therapy. While it is already possible to make a before and after therapy superimposition of one single patient, apparently no previous study created an average dental arch from a group of patients and used it for the same purposes.

The current investigation describes the use of a custom-defined protocol to create a 3D average model of the maxillary dental arch and its validation.

## MATERIALS AND METHODS

A total of 24 upper dental arch models of adult patients were collected for the study. Selection criteria were a full set of permanent teeth from right second molar to left second molar, bilateral Class I molar and canine relationship, absence of major restorations and no previous orthodontic treatment. Average age of the sample was 28.8 years (SD 5.6, range 20-40) and the group consisted of 9 women and 15 men. The study was made in accord with the Declaration of Helsinki and did not involve invasive or dangerous procedures. The study protocol was approved by the local ethic committee (number 12012009-2) and all the analyzed individuals gave their informed consent to the experiment.

Laser-scanned images of the dental cast were obtained with an optical laser-scanning device (D100, Imetric 3D, Courgenay, Swiss). The scanned images were analyzed using the a three-dimensional visualization software (Mirror; Canfield Scientific, Fairfield, NJ). Seventy-nine landmarks were identified on the upper arch on the basis of a protocol previously validated for dental analysis<sup>49,94</sup> (see also chapter 3 of this thesis). A reference plane was computed between the incisive papilla and the intersections of the palatal sulci of the first permanent molars with the gingival margin; this plane is independent from the occlusal plane. The reference plane was mathematically set horizontal with a transverse X axis corresponding to the line connecting the 2 molar landmarks (right-left), a sagittal (anterior-posterior) Y axis, and a vertical (inferior-superior) Z axis. The origin of axes (0, 0, 0) was set at the upper right molar lingual point (Fig. 5.1). All coordinates were rotated and translated according to the new reference system.

The height and length of each tooth together with the intermolar and intercanine distances were calculated as linear measurements. Intermolar distances were calculated both on the vestibular (inter molar V: distance between mesiobuccal cusp tips of the right and left maxillary first molars) and the lingual (inter molar L: distance between the intersections of the palatal sulci of the right and left first permanent molars with the gingival margin). Intercanine distance was calculated as the distance between the right and left cusp tips. The inclination of the Facial Axis of the Clinical Crown (FACC) of each tooth on the reference plane was also calculated as angular measurement (a value lower than 90° means that the tooth is inclined toward the lingual side).

The 3D scans of each dental cast contain the data set of (x,y,z) coordinates that were analyzed to build the average dental arch. We developed an ad hoc multi-platform software system to perform our evaluations. The system is developed by C++ language and based on

the Visualization Toolkit, a widely used freeware open source framework.<sup>95</sup> The digital average dental arch (ADA) shell is obtained by a two steps process: at first dense point-to-point correspondences<sup>96</sup> between a reference dental arch shell and all available 3D scans were found; then the aetic avef Cartesian coordinates of correspondent points was evaluated.

The point-to-point correspondence relationship is obtained with the algorithm proposed by Hu et al.<sup>96</sup> This algorithm is based on the Thin Plate Spline transformation and requires, to be applied, an already known set of corresponding points. The landmarks previously identified on each dental arch are used as input.

The average shape is built starting from the reference template. A preliminary alignment of scans is performed by using the Iterative Closest Point (ICP) algorithm<sup>97</sup> that registers two meshes performing rotation and translation. Then the sum of the coordinates of the correspondent points of all images divided by the number of the images is assigned to each point of the template. Mathematically, if  $r(i,I_j)$  is the point of the  $j$ -th image correspondent to the point  $i$  of the template, the average mesh is the set of point  $p(i)$ :

$$p(i) = \text{Sum}\{j=0\dots N\} r(i,I_j) / N \quad i=0\dots M \text{ (Eq.1)}$$

where  $N$  is the number of available images and  $M$  the number of points in the template image.

A criterion to select the ADA template was defined. After identifying the average coordinates for each single point, the average points were matched with points of each model and the global difference of landmark coordinates was calculated. The dental arch which showed the least difference from the arithmetic average of coordinates of correspondent points was selected as the template for the ADA shell.

To standardize measurements, all data were collected by one experienced investigator and checked by another operator. Measurements were repeated on 10 randomly selected casts to determine the error of the method between the first and second measures. Intraclass correlation coefficients were calculated to compare within-subjects variability to between-subjects variability; all values were larger than 0.95. Standard deviations between repeated measurements were found to be in the range of 0.08 mm to 0.17 mm for linear measurements and between 0.07° and 0.12°. Overall, the method error was considered negligible.

Descriptive statistics were calculated for the traditionally calculated average measurements (TA) deriving from the 24 models. Normal distribution was tested through a Shapiro-Wilk test. All measurements were then matched to their respective expected values (deriving from points used to create the average dental arch) with a one-sample T-test. Significance was set at 5% ( $p < 0.05$ ). The mean of differences (diff) and root mean square (rms) were calculated to express the difference between the measured values and the expected values.

## RESULTS

The height and the length of the dental crowns as well as the inclination of the FACC to the horizontal plane were calculated. Data are reported in Table 5.1. The expected values obtained from the digital 3D average models were not significantly different from the traditionally calculated measurements, with the exception of the angulation of the canines.

The mean difference for linear measurements was  $0.06 \text{ mm} \pm 0.08 \text{ mm}$  (rms  $0.09 \text{ mm}$ ), while larger values were obtained for angular measurements (mean difference,  $-1.14^\circ \pm 2.64^\circ$ , rms  $2.79^\circ$ ).

## DISCUSSION

When new methods for data collection and analysis are introduced into research or clinics, it is mandatory to test their reliability and practical use. In the current investigation, the reliability of the created ADA was tested using well known and documented measurements. Any point of the ADA is the geometric mean of its corresponding points of the single models. Thus linear and angular measurements deriving from the calculated average points can be considered as the expected values. To affirm that the created ADA is a good/realistic 3D-reproduction of the mean of the original dental arches, the expected values have to be as similar as possible to the traditionally calculated mean values.

Statistics showed a very high correspondence of the linear measurements, with a mean difference lower than  $0.1 \text{ mm}$  between the two methods. Angular measurements were also very similar with a mean difference around  $1^\circ$ . When considering angular measurements, the canines showed the highest variability (without the canines the mean angular difference between the two methods was  $-0.19^\circ \pm 1.01$  (rms  $1.01^\circ$ ). When considering the angulation of each tooth there was a clear trend of the premolars and molars for lying toward the lingual side (angulation  $< 90^\circ$ ), while the incisors were in general inclined toward the vestibular side (angulation  $> 90^\circ$ ). For the canines there was not a clear trend since half of them was inclined toward the lingual and the other half laid toward the vestibular side. As all the other measures related to the canines (crown height and length, intercanine distance) were highly reliable, the angular difference may be due to the choice of the reference system. The position of the canine in the dental arch curvature is close to the point of maximum arching and this may require a custom adapted reference system to give better results.

We consider the ADA a good reproduction of reality with some caution in interpreting the canine angulation (which is the only value which was significantly different between the two analyzed measurement sets). It is necessary to further improve the method by testing if missing or erupting teeth can affect the reliability of the ADA.

To find a trusted method to build the ADA is the first step for a new possibility of representing treatment results. At the moment it is possible to match two arches of the same patient before and after therapy and visually interpret the effects by a distance color map. With the chance of building the average arch, the pre-treatment ADA can be matched with the post-treatment ADA and immediately show, better than numbers, the treatment effects. For this purpose a reliable superimposition method should be defined. By far, it seems that the mesial 1/3 of the second palatal rugae and the mesial 2/3 of the third palatal rugae can be a good reference system for the upper dental arches,<sup>38,39,98</sup> while for the lower arch no clear stable points exists (Procrustes method may be the only choice),<sup>99-101</sup> but this was not the purpose of the current investigation.

By extending the number of subjects included into the ADA computation, this methodology may be applied to studies to investigate the variability of the individual arch shape (narrow, wide, ovoid, tapered).

Another possible application of the ADA is matching with a dental arch showing malocclusion. The orthodontist can immediately get the feeling of what is wrong with that malocclusion in terms of discrepancy from an ideal dental arch (Fig. 5.2). By the way an ideal average arch form will never be the aim of an orthodontic treatment, as maxillo-mandibular relationships and a balanced facial profile are the main goals. The ADA could be a useful visual template (selected for ethnicity, gender, age) as the Bolton Standards in cephalometrics<sup>102,103</sup> or the mean faces described by Kau et al.<sup>12,80-83</sup> in stereophotogrammetry.

## CONCLUSIONS

A method for the creation of the Average Dental Arch (ADA) from complete dental arches of adult subjects with sound dentition and no malocclusion was defined and tested for reliability.

The method could be the basis for applications in the orthodontic field like before-after visual comparison to assess treatment effects or as a template for comparison with dental arches showing malocclusion.



## TABLES

**Table 5.1**

Comparison between traditionally calculated average (TA) and expected values of the average dental arch (ADA). For each tooth the height (H, mm) and the length (L, mm) of the crown are reported as well as the inclination (I, deg) with the horizontal (x-y) plane. Transversal distances (mm) were defined in Materials and Methods.  $\Delta$  is the difference between the two sets of measurements.

Tooth	Measure	TA		ADA	TA-ADA		s
		Mean	SD		$\Delta$	P value	
11	H	9.65	1.00	9.60	0.05	0.81	
	L	7.59	0.70	7.40	0.19	0.20	
	I	95.26	7.26	95.25	0.01	0.99	
12	H	7.95	0.71	7.85	0.10	0.50	
	L	5.79	0.82	5.52	0.27	0.12	
	I	96.55	9.20	96.62	-0.06	0.97	
13	H	9.11	0.89	9.04	0.07	0.70	
	L	6.82	0.57	6.64	0.18	0.14	
	I	89.96	11.26	96.44	-6.48	0.01	*
14	H	7.86	0.93	7.79	0.07	0.72	
	L	5.54	0.53	5.53	0.01	0.93	
	I	80.94	8.25	81.29	-0.35	0.83	
15	H	6.88	1.05	6.84	0.04	0.86	
	L	5.43	0.52	5.41	0.02	0.85	
	I	78.96	7.33	79.62	-0.66	0.66	
16	H	5.28	0.54	5.25	0.03	0.79	
	L	8.99	0.70	8.92	0.07	0.63	
	I	77.64	7.02	77.65	-0.01	0.99	
17	H	4.66	0.95	4.56	0.11	0.61	
	L	7.94	1.00	7.86	0.08	0.70	
	I	84.97	12.88	82.55	2.43	0.37	
21	H	9.63	1.27	9.58	0.05	0.85	
	L	7.73	0.60	7.67	0.05	0.63	
	I	94.78	8.24	95.45	-0.67	0.69	
22	H	8.03	0.74	7.93	0.11	0.51	
	L	5.80	0.67	5.65	0.16	0.28	
	I	96.65	9.89	98.53	-1.87	0.36	
23	H	9.30	0.97	9.40	-0.10	0.62	
	L	6.87	0.57	6.80	0.07	0.55	
	I	90.66	11.47	97.93	-7.26	0.00	**
24	H	8.00	1.19	7.95	0.05	0.84	
	L	5.59	0.57	5.54	0.05	0.67	
	I	82.65	7.18	83.06	-0.41	0.78	
25	H	6.75	1.16	6.71	0.05	0.87	
	L	5.32	0.40	5.30	0.02	0.81	
	I	80.29	7.43	81.47	-1.18	0.44	
26	H	5.33	0.93	5.32	0.00	0.96	
	L	9.07	0.76	9.01	0.06	0.70	
	I	78.91	4.39	79.68	-0.76	0.40	
27	H	4.74	0.91	4.71	0.02	0.87	
	L	8.00	1.08	7.93	0.07	0.75	
	I	82.55	11.30	81.24	1.31	0.57	
<b>Transversal Distances (mm)</b>	Inter canine	34.63	2.60	34.75	-0.12	0.82	
	Inter molar V	53.20	2.85	53.26	-0.06	0.92	
	Inter molar L	34.87	1.08	34.90	-0.03	0.89	

P values were obtained from paired Student's t tests; significance (s) was set at 5%: \* p < 0.05, \*\* p < 0.001

## FIGURES

**Figure 5.1**

Occlusal view of the average dental arch and of the digitized landmarks. The reference system is shown in blue.

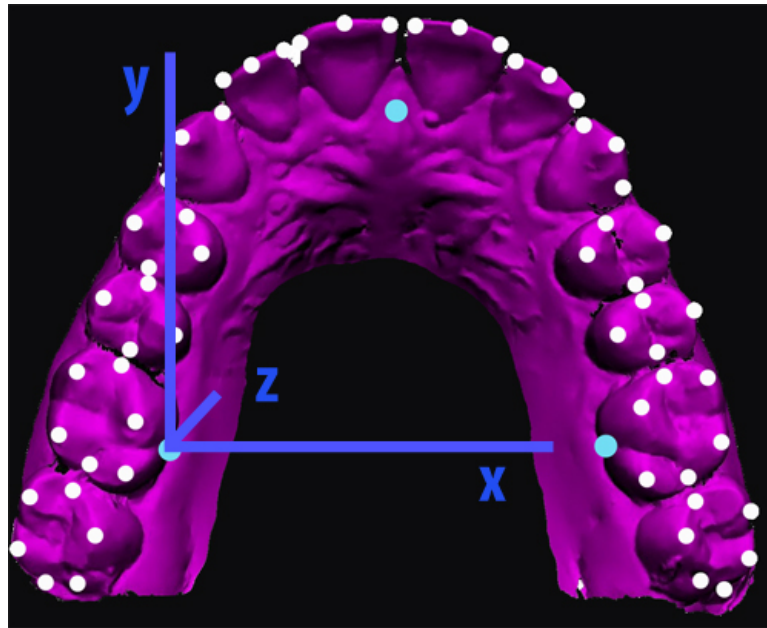
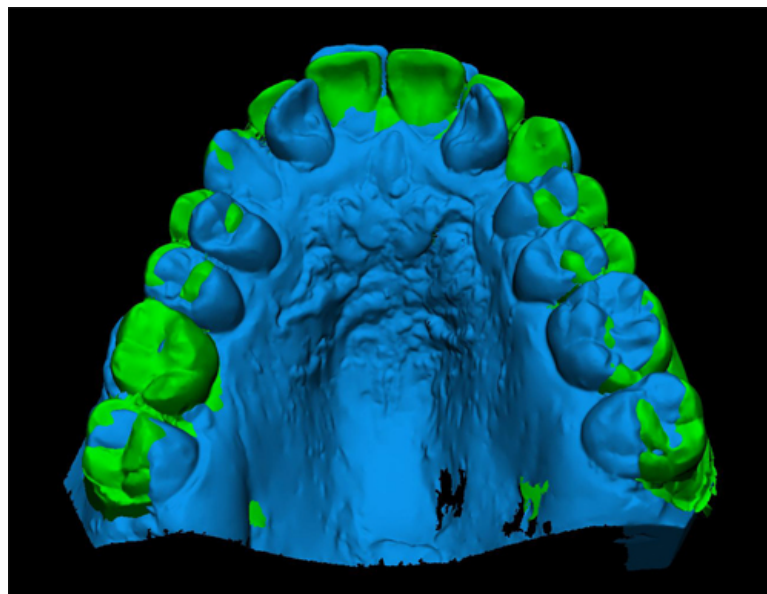


**Figure 5.2**

Average dental arch (green) used as a template for comparison with an arch showing malocclusion (blue).



## **Chapter 6**

---

### **General conclusions**

## GENERAL CONCLUSIONS

Many of the potentialities of three-dimensional dental virtual models have been explored throughout this thesis:

- Storage advantages and sharing facilitation
- Dental analysis showing unconventional measure like tip and torque
- Application of dental analysis to clinical research
- Creation of an average dental arch from as a template of a population

As 3D scanners cost between 10k-15k euros and intraoral scanners cost between 20k-30k euros, the high cost of this technology is the main limit to its diffusion. Despite these limitations, an increasing number of orthodontic labs is providing customers with 3D services.

The likely to come advent of intraoral scanners as a common diagnostic tool in the future will further strengthen the shift from bi-dimensional to three-dimensional diagnosis.

To master virtual study models as they are the main non-invasive diagnostic record, represents a duty for the researcher in the orthodontic field. As the digital divide will decrease between manufacturer/academics and the clinics, the clinicians will also benefit of an everyday usage of three-dimensional virtual dental models.

Integration of 3D images coming from different sources (CBCT, stereophotogrammetry, virtual dental cast) will be likely to become a common scenario. Hopefully merging together bone, skin and dental structures will give clinicians and researchers a more powerful diagnostic tool that allows considering simultaneously the sagittal, transversal and vertical dimensions. As the diagnosis and consequent treatment plans have traditionally been based on bi-dimensional images, the role of academic research is a key factor to drive the orthodontic and dental world to a better understanding of the three-dimensional images.

## **Chapter 7**

---

## **References**

## REFERENCES

1. Kau CH, Richmond S, Incrapera A, English J, Xia JJ. Three-dimensional surface acquisition systems for the study of facial morphology and their application to maxillofacial surgery. *Int J Med Robot.* 2007;3(2):97–110.
2. Kravitz ND, Kusnoto B, BeGole E, Obrez A, Agran B. How well does Invisalign work? A prospective clinical study evaluating the efficacy of tooth movement with Invisalign. *Am J Orthod Dentofacial Orthop.* 2009;135(1):27–35.
3. Lagravère MO, Flores-Mir C. The treatment effects of Invisalign orthodontic aligners: a systematic review. *J Am Dent Assoc.* 2005;136(12):1724–9.
4. Saxe AK, Louie LJ, Mah J. Efficiency and effectiveness of SureSmile. *World J Orthod.* 2010;11(1):16–22.
5. Farronato G, Garagiola U, Dominici A, et al. “Ten-point” 3D cephalometric analysis using low-dosage cone beam computed tomography. *Prog Orthod.* 2010;11(1):2–12.
6. Pauls AH. Therapeutic accuracy of individualized brackets in lingual orthodontics. *J Orofac Orthop.* 2010;71(5):348–61.
7. Yuan T, Liao W, Dai N, Cheng X, Yu Q. Single-Tooth Modeling for 3D Dental Model. *Int J Biomed Imaging.* 2010;2010.
8. Wriedt S, Jaklin J, Al-Nawas B, Wehrbein H. Impacted upper canines: examination and treatment proposal based on 3D versus 2D diagnosis. *J Orofac Orthop.* 2012;73(1):28–40.
9. Holberg C, Steinhäuser S, Geis P, Rudzki-Janson I. Cone-beam computed tomography in orthodontics: benefits and limitations. *J Orofac Orthop.* 2005;66(6):434–44.
10. van Vlijmen OJC, Kuijpers MAR, Bergé SJ, et al. Evidence supporting the use of cone-beam computed tomography in orthodontics. *J Am Dent Assoc.* 2012;143(3):241–52.
11. Heike CL, Upson K, Stuhaug E, Weinberg SM. 3D digital stereophotogrammetry: a practical guide to facial image acquisition. *Head Face Med.* 2010;6:18.
12. Kau CH, Zhurov A, Richmond S, et al. The 3-dimensional construction of the average 11-year-old child face: a clinical evaluation and application. *J Oral Maxillofac Surg.* 2006;64(7):1086–92.
13. Kusnoto B, Evans CA. Reliability of a 3D surface laser scanner for orthodontic applications. *Am J Orthod Dentofacial Orthop.* 2002;122(4):342–8.
14. Keating AP, Knox J, Bibb R, Zhurov AI. A comparison of plaster, digital and reconstructed study model accuracy. *J Orthod.* 2008;35(3):191–201; discussion 175.
15. Dalstra M, Melsen B. From alginate impressions to digital virtual models: accuracy and reproducibility. *J Orthod.* 2009;36(1):36–41; discussion 14.
16. Garino F, Garino B. The OrthoCAD iOC intraoral scanner: A six-month user report. *J Clin Orthod.* 2011;45(3):161–4.
17. Syrek A, Reich G, Ranftl D, et al. Clinical evaluation of all-ceramic crowns fabricated from intraoral digital impressions based on the principle of active wavefront sampling. *J Dent.* 2010;38(7):553–9.
18. Mårtensson B, Rydén H. The holodent system, a new technique for measurement and storage of dental casts.

*Am J Orthod Dentofacial Orthop.* 1992;102(2):113–9.

19. Kuo E, Miller RJ. Automated custom-manufacturing technology in orthodontics. *Am J Orthod Dentofacial Orthop.* 2003;123(5):578–81.

20. Miller RJ, Kuo E, Choi W. Validation of Align Technology's Treat III digital model superimposition tool and its case application. *Orthod Craniofac Res.* 2003;6 Suppl 1:143–9.

21. Marcel TJ. Three-dimensional on-screen virtual models. *Am J Orthod Dentofacial Orthop.* 2001;119(6):666–8.

22. Leifert MF, Leifert MM, Efstratiadis SS, Cangialosi TJ. Comparison of space analysis evaluations with digital models and plaster dental casts. *Am J Orthod Dentofacial Orthop.* 2009;136(1):16.e1–4; discussion 16.

23. Zilberman O, Huggare JAV, Parikakis KA. Evaluation of the validity of tooth size and arch width measurements using conventional and three-dimensional virtual orthodontic models. *Angle Orthod.* 2003;73(3):301–6.

24. Naidu D, Scott J, Ong D, Ho CTC. Validity, reliability and reproducibility of three methods used to measure tooth widths for Bolton analyses. *Aust Orthod J.* 2009;25(2):97–103.

25. Watanabe K, Koga M. A morphometric study with setup models for bracket design. *Angle Orthod.* 2001;71(6):499–511.

26. Kihara T, Tanimoto K, Michida M, et al. Construction of orthodontic setup models on a computer. *Am J Orthod Dentofacial Orthop.* 2012;141(6):806–813.

27. Paniagua B, Cevidanes L, Zhu H, Styner M. Outcome quantification using SPHARM-PDM toolbox in orthognathic surgery. *Int J Comput Assist Radiol Surg.* 2011;6(5):617–26.

28. Hayashi K, Araki Y, Uechi J, Ohno H, Mizoguchi I. A novel method for the three-dimensional (3-D) analysis of orthodontic tooth movement--calculation of rotation about and translation along the finite helical axis. *J Biomech.* 2002;35(1):45–51.

29. Grauer D, Proffit WR. Accuracy in tooth positioning with a fully customized lingual orthodontic appliance. *Am J Orthod Dentofacial Orthop.* 2011;140(3):433–43.

30. Ferrario VF, Sforza C, Colombo A, Ciusa V, Serrao G. Three-dimensional inclination of the dental axes in healthy permanent dentitions--A cross-sectional study in a normal population. *Angle Orthod.* 2001;71(4):257–64.

31. Cattaneo PM, Treccani M, Carlsson K, et al. Transversal maxillary dento-alveolar changes in patients treated with active and passive self-ligating brackets: a randomized clinical trial using CBCT-scans and digital models. *Orthod Craniofac Res.* 2011;14(4):222–33.

32. Primožič J, Perinetti G, Richmond S, Ovsenik M. Three-dimensional longitudinal evaluation of palatal vault changes in growing subjects. *Angle Orthod.* 2011;82(4):632–636.

33. de Menezes M, Rosati R, Ferrario VF, Sforza C. Accuracy and reproducibility of a 3-dimensional stereophotogrammetric imaging system. *J Oral Maxillofac Surg.* 2010;68(9):2129–35.

34. Rosati R, Rossetti A, De Menezes M, Ferrario VF, Sforza C. The occlusal plane in the facial context: inter-operator repeatability of a new three-dimensional method. *Int J Oral Sci.* 2012;4(1):34–7.

35. Thiruvengkatachari B, Al-Abdallah M, Akram NC, Sandler J, O'Brien K. Measuring 3-dimensional tooth movement with a 3-dimensional surface laser scanner. *Am J Orthod Dentofacial Orthop.* 2009;135(4):480–5.

36. Nam S-E, Kim Y-H, Park Y-S, et al. Three-dimensional dental model constructed from an average dental form. *Am J Orthod Dentofacial Orthop*. 2012;141(2):213–8.
37. Björk A. The use of metallic implants in the study of facial growth in children: method and application. *Am J Phys Anthropol*. 1968;29(2):243–54.
38. Jang I, Tanaka M, Koga Y, et al. A novel method for the assessment of three-dimensional tooth movement during orthodontic treatment. *Angle Orthod*. 2009;79(3):447–53.
39. Chen G, Chen S, Zhang XY, et al. Stable region for maxillary dental cast superimposition in adults, studied with the aid of stable miniscrews. *Orthod Craniofac Res*. 2011;14(2):70–9.
40. Khambay B, Nebel J-C, Bowman J, et al. 3D stereophotogrammetric image superimposition onto 3D CT scan images: the future of orthognathic surgery. A pilot study. *Int J Adult Orthodon Orthognath Surg*. 2002;17(4):331–41.
41. Zilberman O, Huggare JAV, Parikakis KA. Evaluation of the validity of tooth size and arch width measurements using conventional and three-dimensional virtual orthodontic models. *Angle Orthod*. 2003;73(3):301–6.
42. Fleming PS, Marinho V, Johal A. Orthodontic measurements on digital study models compared with plaster models: a systematic review. *Orthod Craniofac Res*. 2011;14(1):1–16.
43. Cuperus AMR, Harms MC, Rangel F, et al. Dental models made with an intraoral scanner: A validation study. *Am J Orthod Dentofacial Orthop*. 2012;142(3):308–13.
44. McNamara JAJ, Baccetti T, Franchi L, Herberger TA. Rapid maxillary expansion followed by fixed appliances: a long-term evaluation of changes in arch dimensions. *Angle Orthod*. 2003;73(4):344–53.
45. Andrews LF. *The concept and the appliance*. San Diego: LA Wells Co. 1989.
46. Mestriner MA, Enoki C, Mucha JN. Normal torque of the buccal surface of mandibular teeth and its relationship with bracket positioning: a study in normal occlusion. *Braz Dent J*. 2006;17(2):155–60.
47. Richmond S, Klufas ML, Sywanyk M. Assessing incisor inclination: a non-invasive technique. *Eur J Orthod*. 1998;20(6):721–6.
48. Kannabiran P, Thirukonda GJ, Mahendra L. The crown angulations and inclinations in Dravidian population with normal occlusion. *Indian J Dent Res*. 2012;23(1):53–58.
49. Ferrario VF, Sforza C, Colombo A, Ciusa V, Serrao G. Three-dimensional inclination of the dental axes in healthy permanent dentitions--A cross-sectional study in a normal population. *Angle Orthod*. 2001;71(4):257–64.
50. Lineberger M. Titolo da definire. 2012.
51. Brief J, Behle JH, Stellzig-Eisenhauer A, Hassfeld S. Precision of landmark positioning on digitized models from patients with cleft lip and palate. *Cleft Palate Craniofac J*. 2006;43(2):168–73.
52. Carter GA, McNamara JAJ. Longitudinal dental arch changes in adults. *Am J Orthod Dentofacial Orthop*. 1998;114(1):88–99.
53. Springate SD. The effect of sample size and bias on the reliability of estimates of error: a comparative study of Dahlberg's formula. *Eur J Orthod*. 2012;34(2):158–63.
54. Rosati R, de Menezes M, Rossetti A, Sforza C, Ferrario VF. Digital dental cast placement in 3-dimensional,



- full-face reconstruction: a technical evaluation. *Am J Orthod Dentofacial Orthop.* 2010;138(1):84–88.
55. Luu NS, Nikolcheva LG, Retrouvey J-M, et al. Linear measurements using virtual study models. *Angle Orthod.* 2012;82(6):1098–1106.
56. Thilander B, Wahlund S, Lennartsson B. The effect of early interceptive treatment in children with posterior cross-bite. *Eur J Orthod.* 1984;6(1):25–34.
57. Egermark-Eriksson I, Carlsson GE, Magnusson T, Thilander B. A longitudinal study on malocclusion in relation to signs and symptoms of cranio-mandibular disorders in children and adolescents. *Eur J Orthod.* 1990;12(4):399–407.
58. Bishara SE, Burkey PS, Kharouf JG. Dental and facial asymmetries: a review. *Angle Orthod.* 1994;64(2):89–98.
59. McNamara JA. Maxillary transverse deficiency. *Am J Orthod Dentofacial Orthop.* 2000;117(5):567–70.
60. Moussa R, O'Reilly MT, Close JM. Long-term stability of rapid palatal expander treatment and edgewise mechanotherapy. *Am J Orthod Dentofacial Orthop.* 1995;108(5):478–88.
61. Basciftci FA, Karaman AI. Effects of a modified acrylic bonded rapid maxillary expansion appliance and vertical chin cap on dentofacial structures. *Angle Orthod.* 2002;72(1):61–71.
62. Lima AC, Lima AL, Filho RMAL, Oyen OJ. Spontaneous mandibular arch response after rapid palatal expansion: a long-term study on Class I malocclusion. *Am J Orthod Dentofacial Orthop.* 2004;126(5):576–82.
63. Geran RG, McNamara JA, Baccetti T, Franchi L, Shapiro LM. A prospective long-term study on the effects of rapid maxillary expansion in the early mixed dentition. *Am J Orthod Dentofacial Orthop.* 2006;129(5):631–40.
64. O'Grady PW, McNamara JA, Baccetti T, Franchi L. A long-term evaluation of the mandibular Schwarz appliance and the acrylic splint expander in early mixed dentition patients. *Am J Orthod Dentofacial Orthop.* 2006;130(2):202–13.
65. Baysal A, Veli I, Ucar FI, et al. Changes in mandibular transversal arch dimensions after rapid maxillary expansion procedure assessed through cone-beam computed tomography. *Kor J Orthod.* 2011;41(3):200.
66. Primožic J, Richmond S, Kau CH, Zhurov A, Ovsenik M. Three-dimensional evaluation of early crossbite correction: a longitudinal study. *Eur J Orthod.* 2011:DOI 10.1093/ejo/cjq198.
67. Primožic J, Baccetti T, Franchi L, et al. Three-dimensional assessment of palatal change in a controlled study of unilateral posterior crossbite correction in the primary dentition. *Eur J Orthod.* 2011:DOI 10.1093/ejo/cjr125.
68. Baccetti T, Franchi L, McNamara JA. The Cervical Vertebral Maturation (CVM) Method for the Assessment of Optimal Treatment Timing in Dentofacial Orthopedics. *Sem Orthod.* 2005;11(3):119–129.
69. Cohen J. A power primer. *Psychol Bull.* 1992;112:155–159.
70. Baccetti T, Franchi L, Cameron CG, McNamara J a. Treatment timing for rapid maxillary expansion. *Angle Orthod.* 2001;71(5):343–50.
71. Barrow GV, White JR. Developmental changes of the maxillary and mandibular dental arches. *Angle Orthod.* 1952;22:41–46.
72. Sillman JH. Dimensional changes of the dental arches: Longitudinal study from birth to 25 years. *Am J Orthod.* 1964;50(11):824–842.

73. Bishara SE, Jakobsen JR, Treder J, Nowak A. Arch width changes from 6 weeks to 45 years of age. *Am J Orthod Dentofacial Orthop.* 1997;111(4):401–9.
74. Moorers CF, Reed RB. Changes in dental arch dimensions expressed on the basis of tooth eruption as a measure of biologic age. *J Dent Res.* 1965;44:129–41.
75. Wertz RA. Skeletal and dental changes accompanying rapid midpalatal suture opening. *Am J Orthod.* 1970;58(1):41–66.
76. Sandstrom RA, Klapper L, Papaconstantinou S. Expansion of the lower arch concurrent with rapid maxillary expansion. *Am J Orthod Dentofacial Orthop.* 1988;94(4):296–302.
77. Haas AJ. Rapid expansion of the maxillary dental arch and nasal cavity by opening the midpalatal suture. *Angle Orthod.* 1961;31:73–90.
78. Lagravere MO, Heo G, Major PW, Flores-Mir C. Meta-analysis of immediate changes with rapid maxillary expansion treatment. *J Am Dent Assoc.* 2006;137(1):44–53.
79. Han UK, Vig KW, Weintraub JA, Vig PS, Kowalski CJ. Consistency of orthodontic treatment decisions relative to diagnostic records. *Am J Orthod Dentofacial Orthop.* 1991;100(3):212–9.
80. Gor T, Kau CH, English JD, Lee RP, Borbely P. Three-dimensional comparison of facial morphology in white populations in Budapest, Hungary, and Houston, Texas. *Am J Orthod Dentofacial Orthop.* 2010;137(3):424–32.
81. Kau CH, Zhurov A, Richmond S, et al. Facial templates: a new perspective in three dimensions. *Orthod Craniofac Res.* 2006;9(1):10–7.
82. Kau CH, Richmond S, Savio C, Mallorie C. Measuring Adult Facial Morphology in Three Dimensions. *Angle Orthod.* 2006;76(5):773–78.
83. Seager DC, Kau CH, English JD, et al. Facial morphologies of an adult Egyptian population and an adult Houstonian white population compared using 3D imaging. *Angle Orthod.* 2009;79(5):991–9.
84. Heymann GC, Cevidanes L, Cornelis M, De Clerck HJ, Tulloch JFC. Three-dimensional analysis of maxillary protraction with intermaxillary elastics to miniplates. *Am J Orthod Dentofacial Orthop.* 2010;137(2):274–84.
85. Grauer D, Cevidanes LSH, Proffit WR. Working with DICOM craniofacial images. *Am J Orthod Dentofacial Orthop.* 2009;136(3):460–70.
86. Cevidanes LHC, Heymann G, Cornelis MA, DeClerck HJ, Tulloch JFC. Superimposition of 3-dimensional cone-beam computed tomography models of growing patients. *Am J Orthod Dentofacial Orthop.* 2009;136(1):94–9.
87. Tomassetti JJ, Taloumis LJ, Denny JM, Fischer JR. A comparison of 3 computerized Bolton tooth-size analyses with a commonly used method. *Angle Orthod.* 2001;71(5):351–7.
88. Kuroda T, Motohashi N, Tominaga R, Iwata K. Three-dimensional dental cast analyzing system using laser scanning. *Am J Orthod Dentofacial Orthop.* 1996;110(4):365–9.
89. Stevens DR, Flores-Mir C, Nebbe B, et al. Validity, reliability, and reproducibility of plaster vs digital study models: comparison of peer assessment rating and Bolton analysis and their constituent measurements. *Am J Orthod Dentofacial Orthop.* 2006;129(6):794–803.
90. Ho CT, Freer TJ. A computerized tooth-width analysis. *J Clin Orthod.* 1999;33(9):498–503.

91. Oh Y-H, Park H-S, Kwon T-G. Treatment effects of microimplant-aided sliding mechanics on distal retraction of posterior teeth. *Am J Orthod Dentofacial Orthop*. 2011;139(4):470–81.
92. Jacobson A. The proportionate template as a diagnostic aid. *Am J Orthod*. 1979;75(2):156–72.
93. Kau CH, Cronin AJ, Richmond S. A three-dimensional evaluation of postoperative swelling following orthognathic surgery at 6 months. *Plast Reconstr Surg*. 2007;119(7):2192–9.
94. Ferrario VF, Sforza C, Colombo A, et al. Dental arch size in healthy human permanent dentitions: ethnic differences as assessed by discriminant analysis. *Int J Adult Orthodon Orthognath Surg*. 1999;14(2):153–162.
95. Freeware. Visualization Toolkit (open source). Available at: <http://www.vtk.org/>. Accessed November 14, 2012.
96. Hu Y, Zhou M, Wu Z. A dense point-to-point alignment method for realistic 3D face morphing and animation. *Int J Comp Games Tech*. 2009;2009:1–9.
97. Zhang Z. Iterative point matching for registration of free-form curves and surfaces. *Int J Comp Vis*. 1994;13(2):119–52.
98. Almeida MA, Phillips C, Kula K, Tulloch C. Stability of the palatal rugae as landmarks for analysis of dental casts. *Angle Orthod*. 1995;65(1):43–8.
99. Penin X. Procruste cephalometry. *Orthod Fr*. 2006;77(4):407–15.
100. Goodall C. Procrustes methods in the statistical analysis of shape. *J Royal Stat Soc*. 1991;53(2):285–339.
101. Rohlf FJ, Slice D. Extensions of the Procrustes method for the optimal superimposition of landmarks. *Syst Zool*. 1990;39(1):40.
102. Broadbent B. Bolton Standards and technique in orthodontic practice. *Angle Orthod*. 1937;7(4):209–233.
103. Standerwick RG, Roberts EW, Hartsfield JK, Babler WJ, Katona TR. Comparison of the Bolton Standards to longitudinal cephalograms superimposed on the occipital condyle (I-point). *J Orthod*. 2009;36(1):23–35.

## INDEX OF ABBREVIATIONS

2D	Bi-dimensional
3D	Three dimensional
ADA	Average Dental Arch
BL	Buccal-lingual dimension of a dental crown
CBCT	Cone Beam Computed Tomography
ES	Effect Size
FACC	Facial Axis of Clinical Crown
ICC	Intraclass Correlation Coefficient
ICP	Iterative Closest Point
MD	Mesial-Distal dimension of a dental crown
MME	Method of Moments Estimator
MOT	Months Of Therapy
REM	Relative Error Magnitude
RPE	Rapid Palatal Expander/Expansion
SD	Standard Deviation
T	p-value according to Student T-Test
TA	Traditionally calculated average (when calculating average dental arch)
TB	Transverse Bodily distance between homologous teeth of the same arch
TL	Transvers Lingual distance between homologous teeth of the same arch
TMJ	TemporoMandibular Joint
TV	Transverse Vestibular distance between homologous teeth of the same arch